

# Anomalous and Topological Hall Effects with Phase-Space Berry Curvatures: Electric, Thermal, and Thermoelectric Transport in Magnets

Zachariah Addison,<sup>1,2,\*</sup> Lauren Keyes,<sup>1,\*</sup> and Mohit Randeria<sup>1</sup>

<sup>1</sup>*Department of Physics, The Ohio State University, Columbus, OH 43210, USA*

<sup>2</sup>*Department of Physics and Astronomy, Wellesley College, Wellesley, MA 02482, USA*

(Dated: September 9, 2024)

We develop a theory for the electrical and thermal transverse linear response functions such as the Hall, Nernst and thermal Hall effects in magnetic materials that harbor topological spin textures like skyrmions. In addition to the ordinary transverse response that arises from the Lorentz force due to the external magnetic field, there is an anomalous and a topological response. The intrinsic anomalous response derives from the momentum space Berry curvature arising from the spin-orbit coupling (SOC) in a system with a nonzero magnetization, while the topological response arises from real space Berry curvature related to the topological charge density of the spin texture. To take into account all these effects on an equal footing, we develop a semiclassical theory that incorporates all phase-space Berry curvatures. We calculate the electrical and thermal currents carried by electrons in a system with arbitrary dispersion and general SOC in the presence of arbitrary three-dimensional topological spin textures. We show within a controlled, semiclassical approach that all conductivities – electrical, thermoelectric, and thermal Hall – can be written as the sum of three contributions: ordinary, anomalous and topological, when the conduction electron SOC is weaker than the exchange coupling to the spin texture. All other contributions, including those arising from mixed real-momentum space Berry curvature, are negligible in the regime where our calculations are controlled. We derive various general relations that remain valid, even in the presence of Berry curvatures, at low temperatures including the Weidemann-Franz relation between the electrical and thermal conductivities and the Mott relation between the thermoelectric and electrical conductivities. We also discuss how an in-plane Hall response arises in three-dimensional materials with sufficiently low symmetry. Finally, the Hall response is qualitatively different when the conduction electron SOC is stronger than the exchange coupling to the spin texture, where we find that the anomalous term dominates and the topological term vanishes.

## I. INTRODUCTION

Systems with broken time reversal symmetry host a variety of phases classified by both the symmetry of the system and its topology. The momentum space topology of an insulator in 2D can be characterized by its Hall conductivity, which takes integer values in units of  $e^2/h$ ; the integer is the Chern number, a topological invariant equal to the Brillouin zone integral of the momentum space Berry curvature [1]. The situations in metals with a Fermi surface is different. Ferromagnetic metals exhibit a (non-quantized) anomalous Hall effect [2] proportional to the magnetization, even in the absence of an external magnetic field. In many instances [3], an intrinsic contribution [2, 4–6] to the anomalous Hall effect arising from momentum space Berry curvature dominates over extrinsic contributions from scattering mechanisms involving spin-orbit couplings (SOC).

The Hall effect in systems that harbor topological spin textures is even more interesting. These systems exhibit a topological Hall effect [7–15], typically analyzed as a

signal that appears in addition to an ordinary Hall effect, which scales with the applied magnetic field, and an anomalous Hall effect, which scales with the magnetization. The topological Hall effect is understood to arise from the real space Berry phase [7, 16–20] acquired by conduction electrons moving in a “emergent electromagnetic field” of topological spin textures.

Over the last two decades, a host of magnetic materials [7, 9, 21–23] have been discovered which exhibit topologically nontrivial magnetic textures, including skyrmion crystals, disordered skyrmion arrays, and hedgehog crystals. The most common examples are systems with broken inversion symmetry where the interplay between ferromagnetic exchange and bulk or interfacial Dzyloshinskii-Moriya interaction (DMI) stabilizes skyrmions. Competing interactions other than DMI may also be responsible for stabilizing skyrmions in some centrosymmetric materials [23].

Although the topological Hall effect has by far been the best studied transport signal in magnets with topological spin textures, experiments suggest that thermoelectric and thermal transport also probe the topology of skyrmion phases [24–29]. Materials that harbor isolated skyrmions are promising platforms for novel information storage technologies. This provides a strong motivation for understanding transport in these systems in addition to the fundamental interest in understanding novel Berry phase effects in materials.

---

\* These authors contributed equally

This paper focuses on developing a single unified framework to understand the total Hall response, and its thermal and thermoelectric counterparts, distinct from the separate theoretical approaches for the ordinary, anomalous, and topological contributions that have been used in the past. The semiclassical approach is the natural way to take into account both the momentum-space and real-space Berry curvatures on an equal footing. One then also has to incorporate all phase-space Berry curvatures, as it is not obvious a priori that one can ignore mixed (real- and momentum-space) Berry curvatures. As we shall see, the mixed curvatures are necessary for understanding the thermal counterpart to the electrical Hall response. We build here on our previous work [30, 31] and go beyond it in several ways as discussed at the end of this Section.

In the remainder of this Section we describe the structure of our paper, summarizing our methodology, underlying assumptions, and main results.

In Section II, we introduce our model which describes the dynamics of conduction electrons interacting with local moments. The electrons have an arbitrary band structure with general spin-orbit coupling (SOC), and the local moments form a static spin texture with a specified but arbitrary spatial variation in 3D. We emphasize that the spin texture need not be periodic in space.

For magnetic textures that vary slowly in space on a length scale  $L_s$  that is much larger than the microscopic length scales of the lattice spacing  $a$  or the Fermi wavelength  $1/k_F$ , we can utilize semiclassical techniques [4, 32] to describe the motion of electron wavepackets centered about a point  $(\mathbf{r}, \mathbf{k})$  in phase-space. In Section III, we derive the equations of motion that govern the dynamics of  $(\mathbf{r}(t), \mathbf{k}(t))$  in the presence of phase-space Berry curvatures and an external magnetic field. We also derive here the form of the phase-space volume measure in the presence of arbitrary Berry curvatures.

In Section IV, we determine the electronic distribution function  $f(\mathbf{r}, \mathbf{k})$  to linear order in external perturbations – the electric field  $\mathbf{E}$  and gradients of the chemical potential  $\mu$  and temperature  $T$  – by solving the Boltzmann equation within the relaxation time ( $\tau$ ) approximation.

It is useful to clearly discuss at the outset the small parameters that we use to control our calculations. The semiclassical approach requires that the elastic mean free path  $\ell = v_F \tau$  satisfies  $1/k_F \ll \ell$ , and that the magnetic field is such that the cyclotron energy  $\hbar\omega_c \ll E_F$ , the Fermi energy. In principle  $\ell/L_s$  and  $\omega_c \tau$  can take on any values consistent with the semiclassical inequalities. In practice, however, the Boltzmann equation is much easier to solve when  $\omega_c \tau \ll 1$  and  $\ell \ll L_s$ , and this is the regime that we will focus on in this paper. These assumptions are realistic for many materials [23] that exhibit topological spin textures where  $10 \lesssim L_s \lesssim 500$  nm, while  $1 \lesssim \ell \lesssim 100$  nm given that  $10 \lesssim k_F \ell \lesssim 100$ .

The strength  $\lambda$  of the SOC of the conduction electrons plays an important role in our analysis. Since we are modeling systems where the magnetism arises from

3d transition metal ions, we work in the regime where  $\lambda \ll E_F$  or the hopping  $t$  that sets the scale of the bandwidth. However, the results depend crucially on the ratio of the SOC  $\lambda$  to the exchange coupling  $J$  between conduction electron spins and the local moments forming the topological texture. We show that the anomalous and topological responses are of comparable magnitude in the regime of “weak SOC” where  $\lambda \ll J \lesssim t \sim E_F$ . In the “strong SOC” regime where  $J \ll \lambda \ll t \sim E_F$ , we find that the anomalous Hall response dominates and the effect of the real-space Berry curvature is suppressed for reasons discussed below.

Section V is devoted to a detailed discussion of transport currents that flow in response to an external perturbation; these are the currents that are either measured or applied in experiments. We note that the transport currents are distinct from the total current, which also includes “bound magnetization currents” that exist in equilibrium. The electrical transport current  $\mathbf{j}_{\text{tr}}^e$  has been discussed extensively in the literature [4, 30, 31, 33], where classical electromagnetism is used to identify the bound currents arising from the curl of a magnetization. In practice, the transport current  $\mathbf{j}_{\text{tr}}^e$  is determined from the easier calculation of the total current after the subtraction of the bound magnetization currents.

It is difficult to follow the same method to identify the thermal transport current  $\mathbf{j}_{\text{tr}}^Q$  due to the lack of a canonical definition for an analogous “energy magnetization”. Thermal transport currents are theoretically challenging to calculate as the total current includes in addition bound currents that flow even in equilibrium, arising from spatial gradients of a thermal magnetization [33–35]. Attempts have been made to identify their correct form via derivatives of the free energy with respect to a gravito-magnetic field [36–39]. While in principle this does provide a method for calculating the thermal magnetization, in practice these calculations can be cumbersome even in the simplest crystalline systems. We instead build on the techniques put forth in ref. [40] and identify the bound current from the equilibrium expectation value of the total current operator. This allows us to determine  $\mathbf{j}_{\text{tr}}^Q$  without direct calculation of an energy magnetization.

Using this approach, we calculate in Section VI the electric, thermal, and thermoelectric conductivity tensors, defined in terms of transport currents flowing in linear response to external perturbations. The conductivities are given by

$$\begin{pmatrix} \mathbf{j}_{\text{tr}}^e \\ \mathbf{j}_{\text{tr}}^Q \end{pmatrix} = \begin{pmatrix} \overleftrightarrow{\sigma} & \overleftrightarrow{\alpha} \\ \overleftrightarrow{\beta} & \overleftrightarrow{\kappa} \end{pmatrix} \begin{pmatrix} \mathbf{E} - \frac{1}{e} \nabla_r \mu \\ -\nabla_r T \end{pmatrix}. \quad (1)$$

The Hall effect in the electric  $\overleftrightarrow{\sigma}$ , thermoelectric  $\overleftrightarrow{\alpha}$  electrothermal  $\overleftrightarrow{\beta}$ , and thermal conductivities  $\overleftrightarrow{\kappa}$  is identified as the antisymmetric part of each second-rank tensor. This definition eliminates time reversal-even contributions that may exist in the off-diagonal components

	Longitudinal	Ordinary $\sim B$	Anomalous $\sim \Omega_k$	Topological $\sim \Omega_r$
$\rho / \left( \frac{\hbar}{e^2 k_F} \right)$	$\left( \frac{1}{k_F \ell} \right)$	$\omega_c \tau \left( \frac{1}{k_F \ell} \right)$	$\left( \frac{\lambda}{J} \right)^2 \left( \frac{1}{k_F \ell} \right)^2$	$\left( \frac{1}{k_F L_s} \right)^2$
$\left( \begin{array}{c} \text{Seebeck} \\ \text{or Nernst} \end{array} \right) / \left( \frac{k_B}{e} \right)$	Seebeck $\left( \frac{T}{T_F} \right)$	Nernst $\left( \frac{T}{T_F} \right) (\omega_c \tau)$	Nernst $\left( \frac{T}{T_F} \right) \left( \frac{\lambda}{J} \right)^2 \left( \frac{1}{k_F \ell} \right)$	Nernst $\left( \frac{T}{T_F} \right) \left( \frac{\ell}{L_s} \right)^2 \left( \frac{1}{k_F \ell} \right)$
$\kappa / \left( \frac{k_B^2 T k_F}{\hbar} \right)$ $= \frac{\pi^2}{3} \frac{\hbar}{e^2 k_F} \sigma$	$k_F \ell$	$(\omega_c \tau) (k_F \ell)$	$\left( \frac{\lambda}{J} \right)^2$	$\left( \frac{\ell}{L_s} \right)^2$

FIG. 1. **Summary of results.** Table summarizing the semiclassical results for the resistivity, Seebeck or Nernst signal, and thermal conductivity in the regime where the microscopic length scale  $k_F^{-1} \sim a \ll$  elastic mean free path  $\ell \ll L_s$  the scale of variation of the spin texture, and SOC  $\lambda \ll J$ , the exchange coupling between electrons and spin texture, and  $\lambda \ll$  Fermi energy  $E_F = k_B T_F$ . The longitudinal part of each signal is shown, as well as the ordinary, anomalous, and topological contributions, whose sum yields the total Hall response. The thermal conductivity scales like the electric conductivity as a result of the Weidemann-Franz relation that we derive.

of each tensor. To see this clearly, consider the electrical conductivity  $\overleftrightarrow{\sigma}$ , a second rank tensor which can be written as the sum of a symmetric and an antisymmetric tensor. Onsager reciprocity in the presence of an external magnetic field  $\mathbf{B}$  implies  $\sigma_{ij}(\mathbf{B}) = \sigma_{ji}(-\mathbf{B})$ . Thus, the symmetric part of the conductivity is even in  $\mathbf{B}$ , while its antisymmetric part, which is the Hall response, is odd. This motivates us to define for each conductivity tensor  $\zeta \in \{\sigma, \alpha, \kappa\}$ , the antisymmetric ‘‘Hall pseudovector’’,

$$\zeta_i \equiv \frac{1}{2} \epsilon_{ijk} \zeta_{jk}. \quad (2)$$

For instance, the Hall response measured in the  $xy$ -plane is represented by the  $z$  component of the Hall pseudovector  $\zeta_z = (\zeta_{xy} - \zeta_{yx})/2$ . In what follows, we do not discuss  $\overleftrightarrow{\beta}$  because we find that  $\overleftrightarrow{\beta} = T \overleftrightarrow{\alpha}$ , consistent with Onsager reciprocity, and thus it is not an independent transport coefficient.

Using our semiclassical approach, which is controlled in the regime of small parameters described above, we find that the electric, thermoelectric, and thermal Hall conductivities can be written as the sum of the ordinary, anomalous, and topological contributions, namely

$$\zeta = \zeta^O + \zeta^A + \zeta^T, \quad \zeta \in \{\sigma, \alpha, \kappa\}. \quad (3)$$

The ordinary term  $\zeta^O$  arises from the usual Lorentz force effect of an external magnetic field  $\mathbf{B}$ , and the anomalous term  $\zeta^A$  arises from the momentum-space Berry curvature. The topological contribution  $\zeta^T$  derives

from the real-space Berry curvature, which, in the ‘‘weak SOC’’ limit, is identified with the skyrmion or topological charge density  $\hat{\mathbf{m}}(\mathbf{r}) \cdot \partial_r \hat{\mathbf{m}}(\mathbf{r}) \times \partial_{r_j} \hat{\mathbf{m}}(\mathbf{r})$  of an arbitrary spin texture  $\hat{\mathbf{m}}(\mathbf{r})$ . All other contributions, including those arising from mixed real-momentum space Berry curvature, are negligible in the regime where our calculations are controlled.

In the next two sections, we focus on the implications of our results obtained in the weak SOC regime ( $\lambda \ll J \lesssim t$ ). In Section VII, we derive that the Wiedemann-Franz relation between the electrical and thermal conductivities and the Mott relation between the thermoelectric and electrical conductivities at low temperatures remain valid even in the presence of phase-space Berry curvatures. We next express our results for the conductivities in terms of transport coefficients that are more directly related to experimental measurements, namely the resistivity, and the Seebeck and Nernst coefficients. The scaling of the various transport coefficients with the parameters of our theory are summarized in the table in Fig. 1. In Section VIII, we use our results to explore the possibility of an in-plane Hall response which can arise in three-dimensional materials with sufficiently low symmetry.

We next discuss in Section IX the crucial dependence of our results on  $\lambda/J$ . The previous sections focused primarily on the weak SOC regime where the topological and anomalous Hall responses are comparable. In contrast, we find that in the strong SOC regime ( $J \ll \lambda \ll t$ ), the anomalous Hall response dominates, and the

real-space Berry curvature makes a negligible contribution. To understand this better, we look at the example of a 2D skyrmion crystal (SkX). The real space Berry curvature integrated over the SkX unit cell is the Chern number, so how can this topological invariant change as we go from weak to strong SOC? We show that that this occurs through a gap closing at intermediate  $\lambda/J \sim O(1)$ .

We conclude in Section X with a discussion of open questions and directions for future work. We end this introduction with a comment on how this paper goes beyond our previous work [30, 31] and the work of other authors. Our previous work only considered electrical currents in quasi two-dimensional systems in the absence of an external magnetic field, whereas here, we analyze a general 3D Hamiltonian with arbitrary dispersion and SOC and spin textures with arbitrary 3D spatial variation, and explicitly include the magnetic field in the calculation. In addition to skyrmion lattices or disordered skyrmion arrays, the fully 3D treatment presented here would be applicable to systems such as the hedgehog lattice observed in  $\text{MnSi}_{1-x}\text{Ge}_x$  [41], which could not have been described by previous works. The 3D analysis is also essential for the new insights into the in-plane Hall effect. Most importantly, we present for the first time results for the thermal Hall responses, which required us to derive the correct form of the thermal transport current in topological magnets. This analysis also led to the derivation of the the Wiedemann-Franz relation in the presence of arbitrary phase-space Berry curvatures. Finally, all previous work focused implicitly on the weak SOC limit. We show here that this is in fact essential to obtain comparable anomalous and topological Hall responses. We show that the results in the strong SOC limit are qualitatively different with a vanishing real-space Berry curvature.

## II. MODEL

We consider a 3D system of itinerant electrons interacting with local moments that form a topological spin texture. Our formalism can be used to model bulk metallic magnets and magnetic multilayers that harbor topological spin textures [7, 22, 23], as well as heavy metal/magnetic insulator bilayers [14, 15].

We consider a Hamiltonian of the form

$$\hat{H} = \hat{H}_t + \hat{H}_\lambda + \hat{H}_J \quad (4)$$

where  $\hat{H}_t$  is a tight-binding description of conduction electrons,  $\hat{H}_\lambda$  describes the effect of spin-orbit coupling (SOC) on the itinerant electrons, and  $\hat{H}_J$  takes into account the coupling of the electrons to the magnetic texture. We next elaborate on each of these terms.

The electron kinetic energy is given by

$$\hat{H}_t = - \sum_{ij,\sigma} t_{ij} \hat{c}_{i\sigma}^\dagger \hat{c}_{j\sigma}, \quad (5)$$

where  $\sigma$  labels up/down spins, and the hopping amplitudes  $t_{ij}$  between sites  $i$  and  $j$  describe an arbitrary band structure. The electron density is determined by the Fermi energy  $E_F$ .

The SOC term is given by

$$\hat{H}_\lambda = \frac{\lambda\hbar}{at} \sum_{ij,\mu\nu,\sigma\sigma'} \hat{c}_{i\sigma}^\dagger (\chi_{\mu\nu} \sigma_\mu^{\sigma\sigma'} v_\nu^{ij}) \hat{c}_{j\sigma'}. \quad (6)$$

It describes an arbitrary linear coupling between the velocity  $\mathbf{v}^{ij} = i(\mathbf{r}_i - \mathbf{r}_j)t_{ij}/\hbar$  on a bond  $(i, j)$  and the conduction electron spin  $\boldsymbol{\sigma}$ , defined by a vector of Pauli matrices with matrix elements labelled by  $\sigma, \sigma' \in \{\uparrow, \downarrow\}$ .  $\lambda$  is the strength of the SOC with dimensions of energy,  $a$  is the lattice spacing, and  $t$  the scale of the hopping.

We can take into account various different types of SOC in our analysis with an appropriate choice of the dimensionless matrix  $\chi_{\nu\mu}$  with  $\mu, \nu \in \{x, y, z\}$ . These include the following two familiar examples. If we choose  $\chi_{xy} = -\chi_{yx} = 1$ , with all other components zero, then eq. (6) reduces to  $\sum_{ij,\sigma\sigma'} (\sigma_x^{\sigma\sigma'} v_y^{ij} - \sigma_y^{\sigma\sigma'} v_x^{ij}) \hat{c}_{i\sigma}^\dagger \hat{c}_{j\sigma'}$  and we obtain a Rashba SOC. Similarly, linear Dresselhaus SOC is obtained by choosing  $\chi_{xx} = -\chi_{yy} = 1$  with all other components zero.

The third term in the Hamiltonian of eq. (4)

$$\hat{H}_J = -J \sum_{i,\sigma\sigma'} \hat{\mathbf{m}}(\hat{\mathbf{r}}_i) \cdot (\hat{c}_{i\sigma}^\dagger \boldsymbol{\sigma}^{\sigma\sigma'} \hat{c}_{i\sigma'}) \quad (7)$$

describes the coupling of strength  $J$  between the itinerant electron spin  $\boldsymbol{\sigma}$  and a magnetic texture  $\hat{\mathbf{m}}(\mathbf{r})$ , with  $\hat{m}_x^2(\mathbf{r}) + \hat{m}_y^2(\mathbf{r}) + \hat{m}_z^2(\mathbf{r}) = 1$  at each  $\mathbf{r}$ . We assume that the local moments are static, but can have an arbitrary spatial variation in three dimensions.

We will apply external electric and magnetic fields to our system in the next section when we derive the semiclassical equations of motion for the conduction electrons described by the Hamiltonian of eq. (4). At the end, we will also take into account elastic scattering of the conduction electrons from impurities, characterized by a scattering time  $\tau$  or equivalently a mean free path  $\ell = v_F\tau$ , where  $v_F$  is the Fermi velocity. The last step in our semiclassical transport calculation ( $a \ll \ell$ ) will be the solution of the Boltzmann equation within a relaxation time approximation, and it is here that the time scale  $\tau$  will govern the approach to local equilibrium.

## III. SEMICLASSICAL EQUATIONS OF MOTION

As noted in the Introduction, our goal is to take into account both the momentum space Berry curvature and the real space Berry curvature on an equal footing, and the semiclassical approach is ideally suited for this purpose. We begin by considering electronic wave-packets centered around the point  $\boldsymbol{\xi} = (\mathbf{r}_c, \mathbf{q}_c)$  in six-dimensional phase space, and start by obtaining the equations of motion for  $\boldsymbol{\xi}$ . The semiclassical analysis is justified when

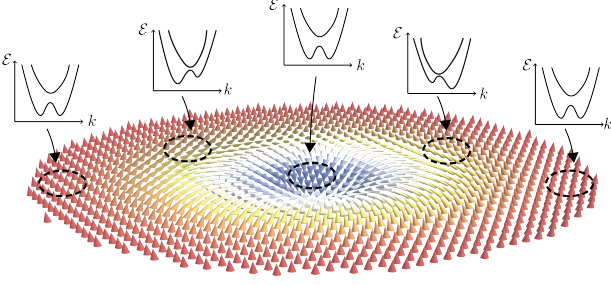


FIG. 2. Schematic illustration of the spatial variation of the local semiclassical band structure at various positions within a topological skyrmion magnetic texture.

there is a clear separation of length scales, so that the lattice spacing and Fermi wavelength  $a \sim k_F^{-1} \ll L_s$ , the characteristic scale of variation the spin texture  $\hat{\mathbf{m}}(\mathbf{r})$  of the local moments, as well as the length scales associated with the external electric and magnetic fields (which are spatially uniform in our problem). The time scale of the magnetic dynamics is also assumed to be much longer than the electronic time scales of the system, which justifies the static magnetic texture treated here. We note in passing that the “skyrmion Hall effect” [7], which involves the motion of spin textures is only seen within non-linear response once the skyrmions are depinned. We focus here only on linear response.

We will find the equations of motion through a standard semiclassical procedure [4, 32]; see Appendix A for details. We start by performing an expansion of  $\hat{H}$  around an arbitrary real-space point  $\mathbf{r}_c$ , to obtain

$$\hat{H} = \hat{H}_c + \Delta\hat{H} \quad (8)$$

where  $\hat{H}_c = \hat{H}(\hat{\mathbf{r}} \rightarrow \mathbf{r}_c)$  and  $\Delta\hat{H}$  is the first order correction, smaller than  $\hat{H}_c$  by a factor of  $a/L_s$ . We will find that the leading order contributions to the transverse electric and thermal responses of the system arise at first order in this expansion, and we neglect terms that are higher order in  $a/L_s$ .

$\hat{H}_c$  has discrete translation symmetry, and may be written in the Bloch basis with eigenstates  $|\psi_{\pm}(\mathbf{r}_c, \mathbf{q})\rangle$  indexed by a crystal momentum  $\mathbf{q}$  and a band index  $\pm$ . It takes the form

$$\begin{aligned} \hat{H}_c &= \varepsilon(\mathbf{q})\mathbb{1} + \mathbf{d}(\mathbf{r}_c, \mathbf{q}) \cdot \boldsymbol{\sigma}, \\ d_{\nu}(\mathbf{r}_c, \mathbf{q}) &= \frac{\lambda}{at} \chi_{\nu\mu} \partial_{q_{\mu}} \varepsilon(\mathbf{q}) - J\hat{m}_{\nu}(\mathbf{r}_c), \end{aligned} \quad (9)$$

where  $\mu, \nu \in \{x, y, z\}$ . The eigenenergies are  $\mathcal{E}_{\pm}(\mathbf{r}_c, \mathbf{q}) = \varepsilon(\mathbf{q}) \pm |\mathbf{d}(\mathbf{r}_c, \mathbf{q})|$ . Denoting the eigenvalues of  $\Delta\hat{H}$  by  $\Delta\mathcal{E}$ , the eigenvalues of the full Hamiltonian  $\hat{H}$  can be written as  $\tilde{\mathcal{E}}_{\pm} = \mathcal{E}_{\pm} + \Delta\mathcal{E}$  to first order in  $a/L_s$ . In Figure 2 we illustrate the spatial variation of the semiclassical eigenvalues at various positions within a topological skyrmion magnetic texture.

We next include the effect of the electromagnetic scalar and vector potentials  $\phi$  and  $\mathbf{A}$  on the conduction electrons. This leads to a shift  $\tilde{\mathcal{E}}_{\pm}(\boldsymbol{\xi}) - e\phi(\mathbf{r}_c, t)$  in the energies and  $\mathbf{k}_c \equiv \mathbf{q}_c + (e/\hbar)\mathbf{A}(\mathbf{r}_c, t)$  in the momenta, where  $e > 0$ .

Using the Bloch states, we construct wave-packets  $|W_{\pm}(\mathbf{r}_c, \mathbf{k}_c)\rangle$  centered about the phase-space point  $(\mathbf{r}_c, \mathbf{k}_c)$ . From now on, we drop the “c” subscript to simplify notation and denote points in phase-space by

$$\boldsymbol{\xi} \equiv (r_x, r_y, r_z, k_x, k_y, k_z). \quad (10)$$

Using the semiclassical Lagrangian

$$L_{\pm}(\boldsymbol{\xi}) = \langle W_{\pm}(\boldsymbol{\xi}) | \left( i\hbar \frac{d}{dt} - \hat{H} \right) | W_{\pm}(\boldsymbol{\xi}) \rangle \quad (11)$$

we obtain the equations of motion [4, 32]

$$\dot{\xi}_{\alpha} = (1/\hbar)(\Gamma^{\pm})_{\alpha\beta}^{-1} \partial_{\xi_{\beta}} [\tilde{\mathcal{E}}_{\pm}(\boldsymbol{\xi}) - e\phi(\mathbf{r}, t)], \quad (12)$$

where the indices  $\alpha, \beta$  label the six components of  $\boldsymbol{\xi}$ . The equations of motion involve the inverse of  $\tilde{\Gamma}^{\pm}$ , a  $6 \times 6$  antisymmetric matrix that encodes information about how the phase-space Berry curvatures and external magnetic field impact the dynamics:

$$\tilde{\Gamma}^{\pm}(\boldsymbol{\xi}) = \begin{pmatrix} \overleftrightarrow{\Omega}_{rr}^{\pm} - \frac{e}{\hbar} \overleftrightarrow{F} & \overleftrightarrow{\Omega}_{rk}^{\pm} - \mathbb{1} \\ \overleftrightarrow{\Omega}_{kr}^{\pm} + \mathbb{1} & \overleftrightarrow{\Omega}_{kk}^{\pm} \end{pmatrix} \quad (13)$$

Here  $F_{ij}$  are the spatial components of the electromagnetic field tensor

$$F_{ij} = \partial_i A_j - \partial_j A_i, \quad (14)$$

with  $i, j \in \{x, y, z\}$  so that, e.g., the magnetic field  $B_z = F_{xy}$ . We note that, in addition to the familiar  $\mathbf{k}$ -space and  $\mathbf{r}$ -space Berry curvatures  $\overleftrightarrow{\Omega}_{kk}$  and  $\overleftrightarrow{\Omega}_{rr}$ , the  $\tilde{\Gamma}^{\pm}$  matrix also includes “mixed-space” Berry curvatures  $\overleftrightarrow{\Omega}_{rk}$  and  $\overleftrightarrow{\Omega}_{kr}$ . The components of the phase-space Berry curvatures, in general, are given by

$$\begin{aligned} \Omega_{\xi_{\alpha}\xi_{\beta}}^{\pm}(\boldsymbol{\xi}) &= s\Omega_{\xi_{\alpha}\xi_{\beta}}, \quad s = \pm 1 \\ \Omega_{\xi_{\alpha}\xi_{\beta}} &= \frac{1}{2} \hat{\mathbf{d}} \cdot (\partial_{\xi_{\alpha}} \hat{\mathbf{d}} \times \partial_{\xi_{\beta}} \hat{\mathbf{d}}). \end{aligned} \quad (15)$$

Using  $\hat{\mathbf{d}} = \mathbf{d}/|\mathbf{d}|$ , it is straightforward to rewrite the above result as  $\Omega_{\xi_{\alpha}\xi_{\beta}} = \mathbf{d} \cdot (\partial_{\xi_{\alpha}} \mathbf{d} \times \partial_{\xi_{\beta}} \mathbf{d})/2|\mathbf{d}|^3$ , which greatly simplifies the Berry curvature calculation for the Hamiltonian of eq. (9).

We have to solve the equations of motion for each band separately but, to simplify notation, we will drop the band index ( $\pm$ ) in the intermediate steps unless it is essential to show it explicitly. We write  $\tilde{\Gamma}^{-1}$  in the compact block form

$$\tilde{\Gamma}^{-1}(\boldsymbol{\xi}) = \frac{1}{\mathcal{D}(\boldsymbol{\xi})} \begin{pmatrix} \overleftrightarrow{\mathbf{K}}(\boldsymbol{\xi}) & \overleftrightarrow{\mathbf{S}}(\boldsymbol{\xi}) \\ -\overleftrightarrow{\mathbf{S}}^T(\boldsymbol{\xi}) & \overleftrightarrow{\mathbf{R}}(\boldsymbol{\xi}) \end{pmatrix} \quad (16)$$

where

$$\mathcal{D}(\boldsymbol{\xi}) \equiv \text{pf } \overleftrightarrow{\Gamma}(\boldsymbol{\xi}) \quad (17)$$

is the pfaffian. We discuss in Appendix A why this particular form, with the pfaffian factored out, is natural for the inverse of an even-dimensional antisymmetric matrix. Specifically for our analysis, we will see that writing  $\overleftrightarrow{\Gamma}^{-1}$  in this form makes transparent the cancellation with the same pfaffian that appears in the phase space volume (see below).

The full expressions for the block matrices appearing in eq. (16) are shown in detail in Appendix A (see eq. (A10)), and involve terms up to quadratic order in Berry curvatures and magnetic field. Some intuition for these matrices can be obtained by examining each to lowest order in Berry curvatures:  $\mathbf{K}_{ij} \approx s\Omega_{k_i k_j}$ ,  $\mathbf{R}_{ij} \approx s\Omega_{r_i r_j} - (e/\hbar)F_{ij}$ , and  $\mathbf{S}_{ij} \approx \delta_{ij}$ .

We can now rewrite the equations of motion (12) as

$$\begin{aligned} \dot{\mathbf{r}} &= \frac{1}{\hbar\mathcal{D}} \left[ \overleftrightarrow{\mathbf{K}} \left( \nabla_r \tilde{\mathcal{E}} + e\mathbf{E} \right) + \overleftrightarrow{\mathbf{S}} \nabla_k \tilde{\mathcal{E}} \right], \\ \dot{\mathbf{k}} &= \frac{1}{\hbar\mathcal{D}} \left[ \overleftrightarrow{\mathbf{R}} \nabla_k \tilde{\mathcal{E}} - \overleftrightarrow{\mathbf{S}}^T \left( \nabla_r \tilde{\mathcal{E}} + e\mathbf{E} \right) \right] \end{aligned} \quad (18)$$

where  $\mathbf{E} = -\partial_t \mathbf{A} - \nabla_r \phi$  is the electric field, and we have suppressed the explicit  $\boldsymbol{\xi}$  dependence of various factors for simplicity. These equations dictate how the phase-space Berry curvatures and external magnetic field impact the semiclassical dynamics of conduction electrons. Here is how some familiar effects appear in these equations. The usual Lorentz force contribution to  $\dot{\mathbf{k}}$  appears through  $\overleftrightarrow{\mathbf{R}} \nabla_k \tilde{\mathcal{E}}$  with the magnetic field coming from  $\overleftrightarrow{\mathbf{R}}$ . Since at leading order in curvatures  $\mathbf{R}_{ij} \approx s\Omega_{r_i r_j} - (e/\hbar)F_{ij}$ , we might expect that the real space Berry curvature will have an effect analogous to a magnetic field, except for the sign change  $s = \pm$  between the two bands. The anomalous velocity term, arising from  $\mathbf{k}$ -space Berry curvature is contained in  $\dot{\mathbf{r}}$  through  $\overleftrightarrow{\mathbf{K}} \nabla_r \tilde{\mathcal{E}}$ .

In the remainder of the paper we use equation (18) together with the Boltzmann equation in a controlled calculation to determine the electric and thermal currents. This calculation will require integration over semiclassical phase space weighted by the phase space measure, so we must determine the correct measure before we can proceed.

**Liouville's Theorem:** According to Liouville's theorem, the phase space volume element must remain invariant under time evolution. In the absence of Berry curvatures, this volume element is simply  $dr_x \wedge dr_y \wedge dr_z \wedge dk_x \wedge dk_y \wedge dk_z$ . However, in the presence of Berry curvatures,  $\mathbf{r}$  and  $\mathbf{k}$  no longer satisfy the canonical Poisson bracket relations, i.e.,  $\{r_i, k_j\} \neq \delta_{ij}$ , and the invariant volume element must be modified [42]. We show here that in general the modified volume element is given by

$$\mathcal{V} = \mathcal{D}(\boldsymbol{\xi}) dr_x \wedge dr_y \wedge dr_z \wedge dk_x \wedge dk_y \wedge dk_z, \quad (19)$$

where  $\mathcal{D}(\boldsymbol{\xi}) \equiv \text{pf } \overleftrightarrow{\Gamma}(\boldsymbol{\xi})$  is the pfaffian of the matrix introduced in eq. (13).

For the special case of a system with *only*  $\mathbf{k}$ -space Berry curvature, the result  $\mathcal{D}(\boldsymbol{\xi}) = 1 + (e/\hbar)\mathbf{B} \cdot \boldsymbol{\Omega}_k$ , with  $\Omega_{k_i} = (1/2)\epsilon_{lmn}\Omega_{k_m k_n}$ , is well known [42] and widely used. The more general result (19) for a system with arbitrary phase-space Berry curvatures is stated without proof in ref. [4]. We present here a simple derivation using standard tools of differential geometry. These may be unfamiliar to some readers and the remainder of this Section may be skipped without impeding understanding of the rest of the paper.

To satisfy Liouville's theorem, the Lie derivative of eq. (19) along flows generated by the velocity field  $\dot{\boldsymbol{\xi}} \equiv \frac{d\boldsymbol{\xi}}{dt}$  must vanish:  $\mathcal{L}_{\dot{\boldsymbol{\xi}}}\mathcal{V} = 0$ . Since  $\dot{\boldsymbol{\xi}} = \sum_{\alpha} \dot{\xi}_{\alpha} \partial_{\xi_{\alpha}} = \frac{d}{dt}$ , we simplify the notation by writing  $\mathcal{L}_t \equiv \mathcal{L}_{\dot{\boldsymbol{\xi}}}$  to indicate that this Lie derivative measures the change of the volume form in time.

We define the two-form  $\omega = \sum_{ij} \Gamma_{ij} d\xi_i \wedge d\xi_j / 2$  and relate it to  $\mathcal{V}$  by noting that  $\mathcal{V} = (\omega \wedge \omega \wedge \omega) / 3!$  as shown in Appendix B. The Lie derivative is  $\mathcal{L}_t \mathcal{V} = \omega \wedge \omega \wedge \mathcal{L}_t \omega$ . We next use the Cartan formula

$$\mathcal{L}_t \omega = i_t(d\omega) + d(i_t \omega), \quad (20)$$

where  $d$  is the exterior derivative and  $i_t$  is the interior product [43]. In Appendix B we show that each term in eq. (20) vanishes; the idea behind this is explained in brief here. We show that  $\omega$  is an exact form by finding an  $\eta$  with the property  $\omega = d\eta$ , and thus the first term obviously vanishes since  $d^2 = 0$ . For the second term, we compute  $d(i_t \omega)$  and use the equation of motion (12) to write it as a product of a symmetric double derivative with an antisymmetric two-form, which also vanishes. This fixes the measure up to an overall multiplicative constant that is determined by noting that  $\mathcal{D}(\boldsymbol{\xi}) = 1$  in the absence of any curvatures.

#### IV. BOLTZMANN EQUATION

Now that we have obtained the equations of motion, the next step in calculating observables within the semiclassical framework is to solve the Boltzmann equation. We will thus obtain the electronic distribution functions  $f^{\pm}(\boldsymbol{\xi})$  that describes the phase space occupation of each band ( $\pm$ ) in the presence of external driving fields. In the semiclassical approach, the band index is a good quantum number and there are no inter-band transitions. We will thus solve for the distribution functions of each band separately, but to simplify notation, we will drop the band index ( $\pm$ ) in the intermediate steps and reinstate it at the end.

In thermodynamic equilibrium, the distribution function is just the Fermi-Dirac distribution:  $f_{\text{eq}}(\boldsymbol{\xi}) = (1 + \exp(\tilde{\mathcal{E}}(\boldsymbol{\xi}) - \mu_0) / k_B T_0)^{-1}$ , where the chemical potential  $\mu_0$  and temperature  $T_0$  determine the number and energy density of the homogeneous system in the absence of any

external perturbations. In a system subjected to thermal or chemical potential gradients, currents are driven by deviations from *local* equilibrium. The local equilibrium distribution  $f_{\text{leq}}(\boldsymbol{\xi})$  also takes the form of the Femi-Dirac distribution  $f_{\text{eq}}(\boldsymbol{\xi})$ , but with a spatially varying chemical potential  $\mu_0 \rightarrow \mu(\mathbf{r})$  and temperature  $T_0 \rightarrow T(\mathbf{r})$ .

The full non-equilibrium distribution  $f(\boldsymbol{\xi})$  can be written as  $f(\boldsymbol{\xi}) = f_{\text{leq}}(\boldsymbol{\xi}) + \delta f(\boldsymbol{\xi})$  where  $\delta f(\boldsymbol{\xi})$  describes deviations from local equilibrium. To calculate currents, we must determine  $\delta f(\boldsymbol{\xi})$ , and to this end we solve the Boltzmann equation

$$\dot{\mathbf{r}} \cdot \nabla_{\mathbf{r}} f(\boldsymbol{\xi}) + \dot{\mathbf{k}} \cdot \nabla_{\mathbf{k}} f(\boldsymbol{\xi}) = - \frac{[f(\boldsymbol{\xi}) - f_{\text{leq}}(\boldsymbol{\xi})]}{\tau}. \quad (21)$$

within a relaxation time approximation. As discussed in the paragraph below eq. (7), the mean free path  $\ell = v_F \tau$  must satisfy  $a \sim k_F^{-1} \ll \ell$ , or equivalently the scattering rate  $\hbar/\tau \ll E_F$  or the bandwidth  $\sim t$ , to ensure the validity of the semiclassical approach.

We are interested here in the linear response to an electric field, temperature gradients, and chemical potential gradients. Solving the Boltzmann equation to first order in external perturbations, we find

$$\delta f = -\tau(1 + \mathbb{P})^{-1} \left[ (\dot{\mathbf{k}}^{(1)} \cdot \nabla_{\mathbf{k}} \tilde{\mathcal{E}} + \dot{\mathbf{r}}^{(1)} \cdot \nabla_{\mathbf{r}} \tilde{\mathcal{E}} - \dot{\mathbf{r}}^{(0)} \cdot \nabla_{\mathbf{r}} \mu) \partial_{\tilde{\mathcal{E}}} + \dot{\mathbf{r}}^{(0)} \cdot \nabla_{\mathbf{r}} T \partial_T \right] f_{\text{eq}} \quad (22)$$

where

$$\mathbb{P} = \tau(\dot{\mathbf{r}}^{(0)} \cdot \nabla_{\mathbf{r}} + \dot{\mathbf{k}}^{(0)} \cdot \nabla_{\mathbf{k}}), \quad (23)$$

and the superscripts on  $\dot{\mathbf{r}}$  and  $\dot{\mathbf{k}}$  refer to the (zeroth or first) order in  $\mathbf{E}$  terms in the equations of motion. A detailed derivation of eq. (22) is given in Appendix C. We note that, once the  $\nabla_{\mathbf{r}} T$  and  $\nabla_{\mathbf{r}} \mu$  terms are explicitly extracted from  $f_{\text{leq}}$ , within linear response we can set  $T(\mathbf{r}) \rightarrow T_0$  and  $\mu(\mathbf{r}) \rightarrow \mu_0$  in the rest of the expression. This is why  $f_{\text{eq}}$  appears on the right hand side of eq. (22).

Formally, the semiclassical result obtained above is valid for arbitrary  $\omega_c \tau$ , provided both the cyclotron energy  $\hbar \omega_c$  and  $\hbar/\tau$  are  $\ll E_F$ , and for arbitrary  $\ell/L_s$ , provided that the lattice spacing  $a \sim k_F^{-1} \ll$  than both the the mean free path  $\ell$  and the spin texture length scale  $L_s$ . The solution of eq. (22) greatly simplifies in the limit of weak fields  $\omega_c \tau \ll 1$  and “slowly varying” spin textures with  $\ell \ll L_s$ .

We proceed as follows. Using  $a \ll L_s$  we can ignore the  $\Delta \mathcal{E}$  correction and write  $\tilde{\mathcal{E}} \simeq \mathcal{E} = \varepsilon(\mathbf{k}) + |\mathbf{d}(\mathbf{r}, \mathbf{k})|$ . We then use the scaling of the derivatives  $\nabla_{\mathbf{r}} \sim (1/L_s)$  and  $\nabla_{\mathbf{k}} \sim a$  together with eq. (18) with  $\mathbf{E} = 0$  to estimate how  $\dot{\mathbf{r}}^{(0)}$  and  $\dot{\mathbf{k}}^{(0)}$  scale in terms of the various small parameters. Substituting this in eq. (23), we see that the contributions to the operator  $\mathbb{P}$  scale at most as  $\omega_c \tau$  or  $\ell/L_s$ . Thus, in the weak-field limit with slowly-varying spin textures, we can make the expansion  $(1 + \mathbb{P})^{-1} = (1 - \mathbb{P} + \dots)$ , a generalization of the classic Zener-Jones analysis, as explained in detail in Appendix C.

We end this Section by presenting results in the regime of weak SOC  $\lambda \ll J \lesssim E_F \sim t$  or bandwidth, which is the main focus of this paper. (See Section IX where we discuss the opposite regime of strong SOC). In the weak SOC regime we can set  $\lambda = 0$ , at leading order in  $a/L_s$  and  $\omega_c \tau$ , in eq. (22) to obtain

$$\delta f \approx \left[ \tau v_i - \hbar \tau^2 (s \Omega_{r_m r_n} - \frac{e}{\hbar} F_{mn}) v_n M_{mi}^{-1} \right] \times \left[ \frac{\varepsilon - \mu_0}{T_0} \partial_{r_i} T + (e E_i - \partial_{r_i} \mu) \right] \partial_{\varepsilon} f_{\text{eq}}. \quad (24)$$

The terms proportional to  $\tau^2$  are the leading order contributions to the transverse conductivities (see Appendix C). Consistent with this limit, we have replaced the energies  $\tilde{\mathcal{E}}_{\pm}(\boldsymbol{\xi})$  with

$$\varepsilon_{\pm}(\mathbf{k}) = \varepsilon(\mathbf{k}) \pm J. \quad (25)$$

In particular,  $f_{\text{eq}}(\tilde{\mathcal{E}}_{\pm}) \rightarrow f_{\text{eq}}(\varepsilon_{\pm})$ , and the velocity and inverse mass tensor are given by

$$v_i \equiv \partial_{k_i} \varepsilon(\mathbf{k})/\hbar; \quad M_{ij}^{-1} \equiv \partial_{k_i} \partial_{k_j} \varepsilon(\mathbf{k})/\hbar^2. \quad (26)$$

## V. CURRENTS

In the absence of external perturbations (temperature gradients, chemical potential gradients, and electric fields), there can still be circulating “bound magnetization currents” *in equilibrium*, that do not contribute to the currents that are either measured or applied in most transport experiments. Following refs. [33, 40], we therefore define the electric (thermal) *transport* current

$$\mathbf{j}_{\text{tr}}^{e(Q)}(\mathbf{r}) = \mathbf{j}^{e(Q)}(\mathbf{r}) - \mathbf{j}_{\text{mag}}^{e(Q)}(\mathbf{r}). \quad (27)$$

as the difference between the total current, given by the expectation values  $\mathbf{j}^{e(Q)}(\mathbf{r}) = \langle \hat{\mathbf{j}}^{e(Q)}(\mathbf{r}) \rangle$  of the electrical (e) or thermal (Q) current operators, and the corresponding “magnetization currents”. Note that these are all current densities, but for simplicity we call them currents. In global equilibrium, we expect the transport currents to vanish, and thus  $\langle \hat{\mathbf{j}}^{e(Q)}(\mathbf{r}) \rangle_{\text{eq}} = \mathbf{j}_{\text{mag}}^{e(Q)}(\mathbf{r})$ . The name “magnetization current” derives from the fact that  $\mathbf{j}_{\text{mag}}^e = \nabla_{\mathbf{r}} \times \mathbf{M}$ , where  $\mathbf{M}$  is the magnetization given by the usual thermodynamic relation  $M_i = -\partial F / \partial B_i$ . In the following, we will identify an analogous “heat magnetization current”.

We will calculate  $\mathbf{j}_{\text{tr}}^{e(Q)}$  as follows. (1) Identify the current operators. (2) Evaluate their expectation values in global equilibrium to find  $\mathbf{j}_{\text{mag}}^{e(Q)}$ . (3) Calculate their expectation values under non-equilibrium conditions and subtract  $\mathbf{j}_{\text{mag}}^{e(Q)}$ . What remains is the transport current.

We now proceed with finding the expressions for  $\mathbf{j}^{e(Q)}(\mathbf{r})$ . The electrical (e) and number (N) current operators are defined by

$$\hat{\mathbf{j}}^e(\mathbf{r}) = -\delta \hat{H} / \delta \mathbf{A}(\mathbf{r}) = -e \hat{\mathbf{j}}^N(\mathbf{r}), \quad (28)$$

and the thermal current operator is given by

$$\widehat{j}^Q(\mathbf{r}) = \widehat{j}^E(\mathbf{r}) - \mu(\mathbf{r})\widehat{j}^N(\mathbf{r}) \quad (29)$$

with

$$\widehat{j}^E(\mathbf{r}) = \frac{1}{2}\{\widehat{H} - e\phi(\mathbf{r}), \widehat{j}^N(\mathbf{r})\}. \quad (30)$$

The expectation values of operators are calculated with the electron wave-packet as described in Appendix A. We use the shorthand notation

$$\int_{\mathbf{k}} \equiv \int \frac{d^3k}{(2\pi)^3}, \quad \int_{\mathbf{r}} \equiv \frac{1}{V} \int d^3r, \quad \text{and} \quad \int_{\xi} \equiv \int_{\mathbf{r}} \int_{\mathbf{k}} \quad (31)$$

where  $V$  is the volume of the system. We also implicitly sum over repeated indices and suppress the  $\xi$ -dependence of quantities. The expectation values are given by

$$\begin{aligned} j^e(\mathbf{r}) &= -e \sum_{\pm} \int_{\mathbf{k}} \left[ \mathcal{D} f \dot{\mathbf{r}} + \nabla_{\mathbf{r}} \times (\mathcal{D} f \mathbf{m}) \right] \\ j^Q(\mathbf{r}) &= \sum_{\pm} \int_{\mathbf{k}} \left[ \mathcal{D} f \dot{\mathbf{r}} \tilde{\mathcal{E}}(\xi) + \nabla_{\mathbf{r}} \times (\mathcal{D} f \mathbf{m} \tilde{\mathcal{E}}(\xi)) \right] \\ &\quad - (e\phi(\mathbf{r}) + \mu(\mathbf{r})) j^N(\mathbf{r}) \end{aligned} \quad (32)$$

where

$$\mathbf{m}_n = \frac{i}{2\hbar} \epsilon_{nij} \langle \partial_{k_i} u | (\widehat{\mathcal{H}}_c - \mathcal{E}) | \partial_{k_j} u \rangle \quad (33)$$

times the electric charge is the orbital magnetic moment of a wave-packet and  $j^N(\mathbf{r}) = -j^e(\mathbf{r})/e$ . The terms containing  $\mathbf{m}(\xi)$  in eq. (32) originate from the finite width of the electron wave-packet that allow contributions to the current deriving from its rotation; see Appendix A and ref. [4].

**Bound Magnetization Currents:** In global equilibrium, when  $f(\xi) = f_{\text{eq}}(\xi)$ ,  $\mu(\mathbf{r}) = \mu_0$ ,  $T(\mathbf{r}) = T_0$ , and  $\phi(\mathbf{r}) = \phi_0$ , the transport current must vanish, and the equilibrium expectation value  $j_{\text{eq}}^{e(Q)}$  is equal to the bound or magnetization current. We thus solve for  $j_{\text{mag}}^{e(Q)}(\mathbf{r})$  by evaluating eq. (32) in global equilibrium, without reference to any thermodynamic definitions of the local magnetizations.

Following ref. [40], the global equilibrium currents are

$$\begin{aligned} j_{\text{eq}}^e(\mathbf{r}) &= -e \nabla_{\mathbf{r}} \times \mathbf{M}_{\text{eq}}^N(\mathbf{r}) \\ j_{\text{eq}}^Q(\mathbf{r}) &= \nabla_{\mathbf{r}} \times \mathbf{M}_{\text{eq}}^E(\mathbf{r}) - (e\phi_0 + \mu_0) \nabla_{\mathbf{r}} \times \mathbf{M}_{\text{eq}}^N(\mathbf{r}). \end{aligned} \quad (34)$$

with

$$\begin{aligned} \mathbf{M}_{\text{eq}}^N(\mathbf{r}) &= \sum_{s=\pm} \int_{\mathbf{k}} \left( \mathcal{D} f_{\text{eq}}(\xi) \mathbf{m}(\xi) + g_{\text{eq}}(\xi) s \Omega_{\mathbf{k}} \right) \\ \mathbf{M}_{\text{eq}}^E(\mathbf{r}) &= \sum_{s=\pm} \int_{\mathbf{k}} \left( \mathcal{D} f_{\text{eq}}(\xi) \tilde{\mathcal{E}}(\xi) \mathbf{m}(\xi) + h_{\text{eq}}(\xi) s \Omega_{\mathbf{k}} \right) \end{aligned} \quad (35)$$

where  $\Omega_{\mathbf{k}}$  is a pseudovector constructed from the  $\mathbf{k}$ -space Berry curvature,  $\Omega_{k_i} \equiv \epsilon_{ijk} \Omega_{k_j k_k} / 2$  and  $s = \pm 1$  for the two bands. Note that for simplicity we have suppressed the band label on all other quantities. See Appendix D for a detailed derivation.

We have also introduced the auxiliary functions

$$\begin{aligned} g_{\text{eq}} &= -k_B T_0 \ln \left( 1 + e^{-(\tilde{\mathcal{E}} - \mu_0)/k_B T_0} \right) \\ h_{\text{eq}} &= - \int_{\tilde{\mathcal{E}}}^{\infty} d\eta \eta f_{\text{eq}} \end{aligned} \quad (36)$$

which have the following relationships to  $f_{\text{eq}}$

$$\frac{\partial g_{\text{eq}}}{\partial \tilde{\mathcal{E}}} = - \frac{\partial g_{\text{eq}}}{\partial \mu_0} = f_{\text{eq}}, \quad \frac{\partial h_{\text{eq}}}{\partial \tilde{\mathcal{E}}} = - \frac{\partial h_{\text{eq}}}{\partial \mu_0} + g_{\text{eq}} = \tilde{\mathcal{E}} f_{\text{eq}}. \quad (37)$$

Eq. (35) follows from eq. (32) by noting that to first order in the Berry curvatures

$$-\partial_{k_j} \mathbf{S}_{ij} = \partial_{r_j} \mathbf{K}_{ij}, \quad (38)$$

where we recall that the  $\mathbf{K}$  and  $\mathbf{S}$  matrices were  $3 \times 3$  blocks of  $\tilde{\Gamma}^{-1}$  in eq. (16). We would like to emphasize again the crucial role, already noted in ref. [40], played by the mixed space Berry curvatures in  $\mathbf{S}$  in determining the form of the equilibrium magnetization and associated equilibrium currents.

By evaluating the currents in global equilibrium, we have identified the magnetization currents. Equilibrium (bound) electric currents take the familiar form as the curl of the magnetization. The heat magnetization current is less familiar [35, 44, 45], but in a similar fashion is defined in terms of the curl of the energy and number magnetizations.

**Transport Currents:** We next evaluate eq. (32) under non-equilibrium conditions, i.e., in the presence of a spatially dependent temperature, chemical potential, and electric potential. As before, the non-equilibrium distribution function deviates from local equilibrium:  $f(\xi) = f_{\text{eq}}(\xi) + \delta f(\xi)$ . We find that the non-equilibrium electric current includes a term  $j_{\text{mag}}^e = -e \nabla_{\mathbf{r}} \times \mathbf{M}_{\text{leq}}^N(\mathbf{r})$  and the heat current contains a term  $j_{\text{mag}}^Q = \nabla_{\mathbf{r}} \times \mathbf{M}_{\text{leq}}^E(\mathbf{r}) - (e\phi(\mathbf{r}) + \mu(\mathbf{r})) \nabla_{\mathbf{r}} \times \mathbf{M}_{\text{leq}}^N(\mathbf{r})$ . We identify these as the magnetization currents existing under non-equilibrium conditions. Note that they have the same form as the equilibrium currents in eq. (34), but with the crucial difference that we must use spatially dependent fields  $\mu(\mathbf{r})$  and  $\phi(\mathbf{r})$ , and *local equilibrium* magnetizations,  $\mathbf{M}_{\text{leq}}^N$  and  $\mathbf{M}_{\text{leq}}^E$ . The local equilibrium magnetizations are similar to those in eq. (35), except that  $f_{\text{eq}} \rightarrow f_{\text{leq}}$ , and the auxiliary functions are similarly altered,  $g_{\text{leq}} = g_{\text{eq}}(\mu_0 \rightarrow \mu(\mathbf{r}), T_0 \rightarrow T(\mathbf{r}))$  and  $h_{\text{leq}} = h_{\text{eq}}(\mu_0 \rightarrow \mu(\mathbf{r}), T_0 \rightarrow T(\mathbf{r}))$ .

Subtracting the magnetization currents from the total nonequilibrium currents allows us to calculate the transport currents to linear order in  $(e\mathbf{E} - \nabla_{\mathbf{r}}\mu)$  and  $\nabla_{\mathbf{r}}T$ . Explicitly writing the band labels  $\pm$  that we had suppressed thus far, we find



$$\mathbf{j}_{\text{tr}}^e(\mathbf{r}) = -\frac{e}{\hbar} \sum_{\pm} \int_{\mathbf{k}} \left[ \delta f^{\pm} \nabla_{\mathbf{k}} \tilde{\mathcal{E}}_{\pm} + \left( s \boldsymbol{\Omega}_{\mathbf{k}} \times \nabla_{\mathbf{r}} T \right) \partial_{T_0} g_{\text{eq}}^{\pm} + s \boldsymbol{\Omega}_{\mathbf{k}} \times (e\mathbf{E} - \nabla_{\mathbf{r}} \mu) \partial_{\mu_0} g_{\text{eq}}^{\pm} \right] \quad (39)$$

$$\mathbf{j}_{\text{tr}}^Q(\mathbf{r}) = \frac{1}{\hbar} \sum_{\pm} \int_{\mathbf{k}} \left[ (\tilde{\mathcal{E}}_{\pm} - \mu_0) \delta f^{\pm} \nabla_{\mathbf{k}} \tilde{\mathcal{E}}_{\pm} + \left( s \boldsymbol{\Omega}_{\mathbf{k}} \times \nabla_{\mathbf{r}} T \right) \partial_{T_0} (h_{\text{eq}}^{\pm} - \mu_0 g_{\text{eq}}^{\pm}) + s \boldsymbol{\Omega}_{\mathbf{k}} \times (e\mathbf{E} - \nabla_{\mathbf{r}} \mu) T_0 \partial_{T_0} g_{\text{eq}}^{\pm} \right]. \quad (40)$$

Up to this point we have not made any assumption about  $\lambda/J$  in this Section. We conclude by focusing on the weak SOC regime with  $\lambda \ll J \lesssim E_F$  or bandwidth. (The strong SOC regime is discussed in Section IX). In this limit, we can make the replacement  $\tilde{\mathcal{E}}_{\pm}(\boldsymbol{\xi}) \rightarrow \varepsilon_{\pm}(\mathbf{k}) = \varepsilon(\mathbf{k}) \pm J$  just as we did in eq. (24). The equilibrium functions  $f_{\text{eq}}$ ,  $g_{\text{eq}}$ , and  $h_{\text{eq}}$  are all functions of  $\varepsilon_{\pm}(\mathbf{k})$ , but from eq. (26) we see that the velocity  $v_i$  and inverse mass tensor  $M_{ij}^{-1}$  are independent of the band label. Reinstating the band labels ( $s = \pm$ ) in the Boltzmann equation solution of eq. (24), we obtain

$$\delta f^{\pm} = \left[ \tau v_i - \hbar \tau^2 (s \Omega_{r_m r_n} - \frac{e}{\hbar} F_{mn}) v_n M_{mi}^{-1} \right] \times \left[ \frac{\varepsilon_{\pm} - \mu_0}{T_0} \partial_{r_i} T + (eE_i - \partial_{r_i} \mu) \right] \partial_{\varepsilon} f_{\text{eq}}^{\pm}. \quad (41)$$

We thus see that the effect of the ‘‘emergent magnetic field’’  $\pm(\hbar/e)\Omega_{r_m r_n}$  from the real space Berry curvature is analogous to the (real) magnetic field  $F_{mn}$  of eq. (14), except for the sign change between the two bands. These  $\delta f^{\pm}$ 's are then substituted into the currents of eqs. (39), (40) to find the conductivities in the next Section.

We note that only the real- and momentum-space Berry curvatures enter the currents defined by eqs. (39), (40), and (41). The mixed space Berry curvature enters the equations of motion through the off-diagonal block in eq. (13), where  $\delta_{ij}$  dominates over  $\Omega_{r_i k_j} \sim (a/L_s)(\lambda/J) \ll 1$ .

The real-space Berry curvature contribution enters  $\delta f^{\pm}$  at zeroth order in SOC. The next correction, arising from the real space derivative of the eigenenergies  $\mathcal{E}_{\pm}$ , scales like  $(\ell/L_s)(\lambda/t)$ . This leads to a term in  $\delta f^{\pm}$  that is proportional to  $\nabla \cdot \hat{\mathbf{m}}$  as shown in (C11). We neglect this contribution in our analysis of the conductivities below, since its volume integral can be rewritten as a boundary term that vanishes for an arbitrary spin texture in the thermodynamic limit. For a periodic structure, such as a skyrmion crystal, this contribution vanishes in every unit cell; see ref. [30].

## VI. CONDUCTIVITIES

We now use spatial average of the local transport currents (39) and (40), together with the solution (41) of the Boltzmann equation to determine the long wavelength electrical ( $\sigma$ ), thermoelectric ( $\alpha$ ), and thermal ( $\kappa$ ) con-

ductivities defined in (1). Note that in the next three Sections we will focus on the weak SOC regime. To present our results compactly, we will use the notation

$$\zeta \in \{\sigma, \alpha, \kappa\} \quad (42)$$

to represent any of the three conductivity tensors. We do not include here the  $\vec{\beta}$  tensor of eq. (1), because it does not contain any independent information. It is easy to see that our results obey the Kelvin relation between the electrothermal and thermoelectric transport coefficients, namely  $\vec{\beta} = T_0 \vec{\alpha}$ . This consistency with the Onsager reciprocal relations also serves as a nontrivial check on our analysis, especially on our expression for the thermal transport current.

Let us first briefly look at the longitudinal response which to leading order is independent of the magnetic field and of all Berry curvature effects in the regime where our results are valid. We find that  $\zeta_{xx} = \tau \sum_{\pm} \int_{\boldsymbol{\xi}} v_x^2 (\partial_{\varepsilon} X_{\pm}^{\zeta})$  where the function

$$X_{\pm}^{\zeta} = \begin{cases} -e^2 f_{\text{eq}}^{\pm} & \text{if } \zeta = \sigma \\ -e \partial_{T_0} g_{\text{eq}}^{\pm} & \text{if } \zeta = \alpha \\ \partial_{T_0} (h_{\text{eq}}^{\pm} - \mu_0 g_{\text{eq}}^{\pm}) & \text{if } \zeta = \kappa \end{cases} \quad (43)$$

Using the results in eq. (36) relating the functions  $g_{\text{eq}}$  and  $h_{\text{eq}}$  to the Fermi function  $f_{\text{eq}}$ , we see that

$$\partial_{\varepsilon} X_{\pm}^{\zeta} = (-\partial f_{\text{eq}}^{\pm} / \partial \varepsilon) Y_{\pm}^{\zeta} \quad (44)$$

where

$$Y_{\pm}^{\zeta} = \begin{cases} e^2 & \text{if } \zeta = \sigma \\ -e (\varepsilon_{\pm} - \mu_0) / T_0 & \text{if } \zeta = \alpha \\ (\varepsilon_{\pm} - \mu_0)^2 / T_0 & \text{if } \zeta = \kappa \end{cases} \quad (45)$$

These are the natural prefactors for the velocities in the charge-charge, charge-heat, and heat-heat current correlations. We thus recover the standard results

$$\zeta_{xx} = \tau \sum_{\pm} \int_{\mathbf{k}} \left( -\frac{\partial f_{\text{eq}}^{\pm}}{\partial \varepsilon} \right) Y_{\pm}^{\zeta} v_x^2 \quad (46)$$

where  $\int_{\boldsymbol{\xi}}$  reduces to  $\int_{\mathbf{k}}$  since there is no spatial dependence to the integrand. Here and below,  $(-\partial f_{\text{eq}}^{\pm} / \partial \varepsilon) \simeq \delta(\varepsilon_{\pm} - \mu_0)$  restricts  $\int_{\mathbf{k}}$  to the Fermi surface in the low temperature regime  $T_0 \ll \mu_0$ .

We next turn to the transverse response, the main focus of our work. We see that the transport currents have two distinct types of contributions: (i) an “extrinsic” contribution that involves the scattering time  $\tau$ , which enters through  $\delta f^\pm$  in the first term of eqs. (39) and (40), and (ii) an “intrinsic” contribution independent of  $\tau$ , coming from the second and third terms in each of the expressions. The external magnetic field and real space Berry curvature enter  $\mathbf{j}_{\text{tr}}^{e(Q)}$  only through  $\delta f^\pm$  and the corresponding “extrinsic” terms give rise to the ordi-

nary and topological responses respectively. The  $\mathbf{k}$ -space Berry curvature, on the other hand, enters through the “intrinsic” terms and leads to the anomalous response. The form of eqs. (39), (40), and (41) clearly shows that there are three contributions – ordinary, topological, and anomalous – to the currents and hence to the conductivities as well. We now show this in detail.

As discussed in the Introduction, the Hall conductivities can be compactly represented by the pseudovector  $\zeta$ . From eqs. (39) and (40) we see that

$$\zeta_i = \sum_{\pm} \int_{\xi} \left[ \frac{\hbar\tau^2}{2} \epsilon_{ijk} \epsilon_{lmn} (\partial_\epsilon X_{\pm}^\zeta) v_j M_{km}^{-1} v_n \left( s \Omega_{r_l} - \frac{e}{\hbar} B_l \right) + \frac{X_{\pm}^\zeta}{\hbar} s \Omega_{k_i} \right] \quad (47)$$

where  $i, j, k, l, m, n \in \{x, y, z\}$ , we have written both real and momentum-space Berry curvatures as pseudovectors, and where  $X_{\pm}^\zeta$  is defined in eq. (43). We thus see that the Hall conductivities in eq. (47) can be written as the sum of three pieces

$$\zeta = \zeta^O + \zeta^A + \zeta^T. \quad (48)$$

where the ordinary  $\zeta^O$  term depends upon the external magnetic field  $\mathbf{B}$ , the anomalous  $\zeta^A$  term on the momentum space Berry curvature,  $\mathbf{\Omega}_{\mathbf{k}}$ , and the topological  $\zeta^T$  term on the real space Berry curvature,  $\mathbf{\Omega}_{\mathbf{r}}$ . This justifies the additive decomposition of the experimental signals into these three parts in the regime of validity of our analysis:  $k_F \sim a \ll \ell = v_F \tau \ll L_s$  with  $\hbar\omega_c \ll \hbar/\tau \ll E_F$  and  $\lambda \ll J \sim E_F$ . The reason why mixed Berry curvatures make a negligible contribution to the final result for transport in this regime was discussed at the end of the previous section; see below eq. (41).

We next show that these three terms can be written as

$$\begin{aligned} \zeta^O &= \tau^2 \overleftrightarrow{G}^\zeta \overline{\mathbf{B}}, \\ \zeta^A &= \overleftrightarrow{F}^\zeta \mathbf{\Lambda}, \\ \zeta^T &= \hbar\tau^2 \overleftrightarrow{F}^\zeta \mathbf{n}^{\text{sk}}. \end{aligned} \quad (49)$$

Here each expression is written as a product of a tensor  $\overleftrightarrow{G}^\zeta$  or  $\overleftrightarrow{F}^\zeta$  that depends only on the band structure, with an appropriate pseudovector  $\overline{\mathbf{B}}$ ,  $\mathbf{\Lambda}$ , or  $\mathbf{n}^{\text{sk}}$ , all of which are defined below. Let us discuss each contribution in turn.

**Ordinary response:**  $\zeta^O$  is the term in  $\zeta$  that is proportional to the external magnetic field, e.g., related to the “ordinary”  $\sigma_{xy}$ ,  $\alpha_{xy}$ , or  $\kappa_{xy}$ . In eq. (49), the spatial average  $\overline{\mathbf{B}} = \int_{\mathbf{r}} B(\mathbf{r})$  is simply  $\mathbf{B}$  for a uniform magnetic field. Here we have split the  $\int_{\xi}$  appearing in eq. (47) into an  $\int_{\mathbf{r}}$  that enters the definition of the pseudovector, and  $\int_{\mathbf{k}}$  that enters  $\overleftrightarrow{G}^\zeta$  defined below, since the leading order contributions to the latter are only functions of  $\mathbf{k}$  through the energies  $\epsilon_{\pm}(\mathbf{k})$ . (This separation of the real

and momentum space integrals works in exactly the same way in the topological and anomalous terms as well). We thus see that

$$G_{il}^\zeta = \frac{e}{2} \epsilon_{ijk} \epsilon_{lmn} \sum_{\pm} \int_{\mathbf{k}} \left( -\frac{\partial f_{\text{eq}}^\pm}{\partial \epsilon} \right) Y_{\pm}^\zeta v_j M_{km}^{-1} v_n \quad (50)$$

which depends only on the band structure through the band velocity  $v_i$  and band curvature  $M_{km}^{-1}$ , defined in eq. (26), and  $Y_{\pm}^\zeta$  defined in eq. (45).

**Topological response:** The topological contribution  $\zeta^T$  is similar to the ordinary one, but with some crucial differences. The “emergent electromagnetic field” is given by ( $2\pi$  times) the flux quantum  $h/e$  multiplied by the pseudovector  $\mathbf{n}^{\text{sk}}$  whose components are given by the topological charge – or skyrmion – density in the  $yz$ ,  $zx$ , and  $xy$  planes:

$$n_i^{\text{sk}} = \epsilon_{ijk} \epsilon_{lmn} \frac{1}{V} \int d^3r \hat{m}_l(\mathbf{r}) \partial_{r_j} \hat{m}_m(\mathbf{r}) \partial_{r_k} \hat{m}_n(\mathbf{r}). \quad (51)$$

The tensor  $F_{il}^\zeta$  appearing in eq. (49) is given by

$$F_{il}^\zeta = \frac{1}{2} \epsilon_{ijk} \epsilon_{lmn} \sum_{\pm} s \int_{\mathbf{k}} \left( -\frac{\partial f_{\text{eq}}^\pm}{\partial \epsilon} \right) Y_{\pm}^\zeta v_j M_{km}^{-1} v_n. \quad (52)$$

with the  $\mathbf{k}$ -space integrals dominated by states near the Fermi surface. In fact the integrals in  $F_{il}^\zeta$  are identical to those in  $G_{il}^\zeta$ , however, unlike eq. (50) there is a relative sign  $s = \pm 1$  between the contributions of the two bands originating from the sign change of the Berry curvature in eq. (15). This sign change between bands in  $F_{il}^\zeta$  has important observable consequences. It leads to, for instance, the avoidance of a Sondheimer cancellation in the topological (and also anomalous) Nernst effects, as noted in Ref. [31].

**Anomalous response:** There are two important questions about the form of  $\zeta^A$  in eq. (49). What is the pseudovector  $\mathbf{\Lambda}$ ? And why does  $\zeta^A$  involve the same  $F_{il}^\zeta$

tensor as the topological term? The latter is far from obvious by looking at the anomalous and topological contributions in eq. (47).

We briefly sketch here how we obtain the anomalous response in eq. (49), with details of the lengthy algebra relegated to Appendix E. For concreteness, we focus on the anomalous Hall effect  $\sigma_i^A$ ; the strategy for  $\alpha_i^A$  and  $\kappa_i^A$  is similar. We see from the last term in eq. (47) that

$$\sigma_i^A = -(e^2/\hbar) \sum_{\pm} s \int_{\xi} f_{\text{eq}}^{\pm} \Omega_{k_i}. \quad (53)$$

We substitute into this result the Berry curvature  $\Omega_{k_i} = \frac{1}{4} \epsilon_{ijk} \epsilon_{lmn} \hat{d}_l (\partial_{k_j} \hat{d}_m) (\partial_{k_k} \hat{d}_n)$  calculated using the  $\hat{\mathbf{d}}$ -vector of eq. (9) for  $\lambda \ll J$ . This leads to

$$\begin{aligned} \sigma_i^A &= \frac{e^2 \hbar^3}{4} \left( \frac{\lambda}{Jat} \right)^2 \epsilon_{ijk} \epsilon_{lmn} \chi_{m\mu} \chi_{n\nu} \\ &\times \int_{\mathbf{r}} \hat{m}_l(\mathbf{r}) \sum_{\pm} s \int_{\mathbf{k}} f_{\text{eq}}^{\pm} M_{j\mu}^{-1} M_{k\nu}^{-1} \end{aligned} \quad (54)$$

where the effective masses arise from the  $\mathbf{k}$ -space derivatives of band velocities. We then manipulate the  $\int_{\mathbf{k}}$  term using integration by parts and exploiting the antisymmetric  $\epsilon$ -tensors as shown in Appendix E we obtain

$$\begin{aligned} \sigma_i^A &= \frac{e^2 \hbar^3}{8} \left( \frac{\lambda}{Jat} \right)^2 \epsilon_{ijk} \epsilon_{lmn} \epsilon_{\gamma\alpha\beta} \epsilon_{\gamma\mu\nu} \chi_{m\alpha} \chi_{n\beta} \int_{\mathbf{r}} \hat{m}_l(\mathbf{r}) \\ &\times \sum_{\pm} s \int_{\mathbf{k}} \left( -\frac{\partial f_{\text{eq}}^{\pm}}{\partial \varepsilon} \right) v_j M_{k\nu}^{-1} v_{\mu} = F_{ij}^{\sigma} \Lambda_j, \end{aligned} \quad (55)$$

with the  $F_{ij}^{\sigma}$  of eq. (52) and  $\Lambda_j$  defined below. A general prescription for writing the anomalous Hall result (53) in a metallic ferromagnet as a Fermi surface integral was given in ref. [5]. The derivation above achieves the same goal for a system with an arbitrary spatially varying magnetization.

Using a similar procedure, all three anomalous transverse conductivities can be written in the form  $\zeta^A = \overleftrightarrow{\mathbf{F}}^{\zeta} \mathbf{\Lambda}$  where the pseudovector

$$\Lambda_i = \frac{\hbar^3}{4} \left( \frac{\lambda}{Jat} \right)^2 \epsilon_{ijk} \epsilon_{lmn} \chi_{mj} \chi_{nk} \int_{\mathbf{r}} \hat{m}_l(\mathbf{r}). \quad (56)$$

To get a better feel for  $\mathbf{\Lambda}$ , let us look at some specific examples. For Rashba SOC, described below eq. 6, we find  $\mathbf{\Lambda}^R = \hbar^3 (\lambda/Jat)^2 \bar{m}_z \hat{z}$ , where  $\bar{m}_z$  indicates a spatial average of the  $z$  component of the magnetization, a result reported earlier [30]. For the linear Dresselhaus SOC, with  $\chi_{xx} = 1$ ,  $\chi_{yy} = -1$ , and zeroes elsewhere,  $\mathbf{\Lambda}^D = -\hbar^3 (\lambda/Jat)^2 \bar{m}_z \hat{z}$ . In order for the  $x$  and  $y$  components of the magnetization to come into play, there must be nonzero SOC along the  $z$ -direction. For instance, Ising SOC combined with Rashba SOC would require the nonzero component  $\chi_{zz} = 1$  in addition to the Rashba components. One then finds  $\mathbf{\Lambda}^{R+I} = \hbar^3 (\lambda/Jat)^2 (\bar{m}_y \hat{x} - \bar{m}_x \hat{y} + \bar{m}_z \hat{z})$ . In essence,  $\mathbf{\Lambda}$  relates the anomalous conductivities to components of the magnetization, in accordance with the SOC present in the system.

## VII. TRANSPORT COEFFICIENTS

We now discuss various aspects of our results. First, we discuss the general relations between various transport coefficients that are well known in the theory of metals. We show that these continue to remain valid in the presence of momentum and real space Berry curvatures. Second, we relate our results for the electrical and thermoelectric conductivities, which are the natural quantities to compute theoretically, to the resistivity, and the Seebeck and Nernst coefficients, which are the natural quantities that experimentalists measures.

### Kelvin, Mott, and Wiedemann-Franz relations:

We discuss here some general relations between the electrical, thermal, and thermoelectric transport coefficients that can be seen from our results. First, Onsager reciprocity mandates that the Kelvin relation  $\overleftrightarrow{\beta} = T_0 \overleftrightarrow{\alpha}$  be obeyed between the electrothermal and thermoelectric tensors defined in eq. (1). It is straightforward to check that this relation is indeed obeyed in our calculations.

Second, ordinary metals exhibit the Mott relation between the thermoelectrical and electrical conductivity tensors at low temperatures. We see from our results that, even in the presence of arbitrary Berry curvatures, the anomalous and topological terms individually obey the Mott relation

$$\overleftrightarrow{\alpha}^{T(A)} = \frac{\pi^2 k_B^2 T}{3 e} \frac{\partial}{\partial \mu} \overleftrightarrow{\sigma}^{T(A)} \quad (57)$$

at low temperatures as noted in ref.[31]; see Appendix F for details.

Next, we show the validity of the Wiedemann-Franz (WF) relation between the thermal and electrical transport coefficients. The anomalous and topological terms individually satisfy

$$\overleftrightarrow{\kappa}^{T(A)} = \frac{\pi^2 k_B^2 T}{3 e^2} \overleftrightarrow{\sigma}^{T(A)} \quad (58)$$

at low temperatures. We sketch here a brief outline of this proof with details described in Appendix F.

We find it convenient here to write the conductivity as a sum of ‘‘intrinsic’’ and ‘‘extrinsic’’ terms, in parallel with contributions to the transport currents described in the paragraph below eq. (46). As noted there, the ‘‘intrinsic’’ term depends on the  $\mathbf{k}$ -space Berry curvature and leads to the anomalous response, while the ‘‘extrinsic’’ term depends on the external magnetic field and real space Berry curvature and leads to the sum of the ordinary and topological responses.

For both types of contributions, it is best to change variables to write the response functions in terms of integral functions of an energy scale  $\eta$  rather than just an integral over the phase space variables  $\xi$ . The response functions each take the form of a phase space integral of the product of some  $\xi$  dependent function,  $S(\xi)$ , and some function that depends only on the energy,  $P(\varepsilon(\xi))$ . We may rewrite this product as

$$P(\varepsilon(\boldsymbol{\xi}))S(\boldsymbol{\xi}) = \int d\eta \partial_\eta \Theta(\eta - \varepsilon(\boldsymbol{\xi}))P(\eta)S(\boldsymbol{\xi}). \quad (59)$$

For the “extrinsic” contributions,  $P(\eta)$  is peaked around  $\mu_0$  for  $k_B T_0 \ll E_F$ . For the “intrinsic” contributions we integrate by parts and note that  $\partial_\eta P(\eta)$  is also peaked around the Fermi energy at low temperatures. Expansions of these terms can be performed around  $\mu_0$  to show that the WF relation is satisfied for both the intrinsic and extrinsic pieces (see Appendix F for details).

**Resistivity and Nernst Coefficient:** It is straightforward to express our results in terms of the experimentally measured resistivity, Seebeck coefficient, and Nernst coefficient. The dependence of the resistivities, Seebeck and Nernst effects, and the thermal conductivity on the parameters of our theory is derived in Appendix G and summarized in the Introduction; see Fig. 1. The resistivity tensor is given by  $\overleftrightarrow{\rho} = \overleftrightarrow{\sigma}^{-1}$ , and thus in 2D, for instance, we get  $\rho_{xx} \simeq 1/\sigma_{xx}$  and  $\rho_{xy} \simeq \sigma_{xy}/\sigma_{xx}^2$  since  $\sigma_{xx} \gg \sigma_{xy}$ .

The Seebeck and Nernst coefficients are given by components of the matrix  $\overleftrightarrow{S} = \overleftrightarrow{\sigma}^{-1} \overleftrightarrow{\alpha}$ . Using the argument of the previous paragraph and the Mott relation, we find that  $N_{xy} \approx -(\pi^2/3)(k_B^2 T/e)(\partial/\partial\mu_0)(\sigma_{xy}/\sigma_{xx})$  for each of the ordinary, anomalous, and topological Nernst coefficients. As pointed out in [31], the ordinary Nernst effect is highly suppressed in the relaxation time approximation. This Sondheimer cancellation [46] is avoided in the anomalous and topological Nernst effects due to the opposite signs of Berry curvatures in the two bands of this spin-split model.

### VIII. IN-PLANE HALL EFFECT

We now turn to a discussion of the ordinary, anomalous, and topological *in-plane Hall effects* (IPHE). These Hall effects arise from a magnetic field  $\mathbf{B}$  or effective magnetic field that lies parallel to the plane in which the Hall effect is measured, namely, the plane spanned by a unit vector that points in the direction  $\nabla T$ ,  $\nabla\mu$ , or  $\mathbf{E}$  and a unit vector that points in the direction of the applied currents. This is in contrast to the usual “out of plane” Hall effect (OPHE), in which  $\mathbf{B}$  is applied perpendicular to this measurement plane. We would like to emphasize that the IPHE is a genuine Hall effect deriving from the antisymmetric part of the conductivity tensor (eq. (2)) that is odd under time reversal ( $\mathbf{B} \rightarrow -\mathbf{B}$ ). It is distinct from what is often termed a “planar Hall effect”, which contributes to the symmetric part,  $\zeta_{ij} + \zeta_{ji}$ , and is even under time reversal.

The IPHE has garnered great experimental interest in recent years. The ordinary IPHE has been reported in  $\text{RuO}_2$  [47], but most experimental studies have focused on the anomalous and topological IPHEs [48–54]. We shall therefore briefly discuss the conditions which are required for these two effects, as captured by Eq. (49).

Both the anomalous and topological IPHEs require that there be an effective magnetic field ( $\mathbf{\Lambda}$  or  $\mathbf{n}^{\text{sk}}$ , respectively) lying in the plane. In the case of the topological IPHE, this amounts to requiring that there be a nonzero skyrmion density lying in the planes perpendicular to the plane of measurement. This depends solely on the magnetic texture, and could be satisfied, for example, by skyrmion tubes lying in the measurement plane or by 3D magnetic hedgehogs [55–57]. In the anomalous IPHE, the orientation of  $\mathbf{\Lambda}$  depends on both the SOC and the magnetic texture, as revealed by the expression for  $\mathbf{\Lambda}$  given in Eq. (56). For example, Rashba SOC,  $(\mathbf{k} \times \hat{z}) \cdot \boldsymbol{\sigma}$ , combined with a ferromagnetic texture  $\hat{\mathbf{m}} = \hat{z}$ , results in  $\mathbf{\Lambda} \parallel \hat{z}$ . However, Rashba SOC which breaks both x- and z-mirror symmetries, such as  $(\mathbf{k} \times (\hat{z} + \hat{x})) \cdot \boldsymbol{\sigma}$ , coupled to  $\hat{\mathbf{m}} = \hat{z}$ , results in nonzero in-plane components of  $\mathbf{\Lambda}$ .

In addition to an in-plane effective magnetic field, the anomalous and topological IPHEs require nonzero off-diagonal components of  $\overleftrightarrow{F}^\zeta$ . By inspecting Eq. (52), we see that this IPHE arises from an effective Lorentz force caused by in-plane components of the effective magnetic field. The IPHE described by this theory can only appear in 3D materials, because this effective Lorentz force is forbidden in 2D. In addition, the off-diagonal components of  $\overleftrightarrow{F}^\zeta$  are only permitted in low symmetry crystals [58].

Going beyond symmetry constraints on the IPHE, one might wonder about the relative strength of the in-plane effects and the more traditional OPHE. For the electrical Hall conductivity, the IPHE vanishes for a spherical Fermi surface, and a small perturbation to the dispersion that breaks the isotropy of the Fermi surface leads to a ratio of the IPHE to OPHE that scales with the size of this perturbation. Therefore, low symmetry crystals with elongated elliptical Fermi surfaces possess a greater opportunity to observing large IPHEs. We leave for future work the full exploration of the parameter space where IPHEs can be significant.

### IX. WEAK VERSUS STRONG SOC

Finally, we discuss how the results presented above change as a function of  $\lambda/J$ . Up to this point, we have focused on the weak SOC regime  $\lambda \ll J \lesssim t \sim E_F$ . We now show that the results are qualitatively different in the strong SOC regime  $J \ll \lambda \ll t \sim E_F$ .

To see this in the simplest setting, we focus on a 2D system with parabolic dispersion and Rashba SOC, although the results are more general. For this system the Hamiltonian of eq. (9) is defined by

$$\mathbf{d} = (\lambda k_y a - J \hat{m}_x(\mathbf{r}), -\lambda k_x a - J \hat{m}_y(\mathbf{r}), -J \hat{m}_z(\mathbf{r})) \quad (60)$$

where the spin texture satisfies  $\hat{m}_x^2(\mathbf{r}) + \hat{m}_y^2(\mathbf{r}) + \hat{m}_z^2(\mathbf{r}) = 1$ . The semiclassical band structure is  $\mathcal{E}_\pm = \hbar^2 k^2 / 2m^* \pm d$ , with effective electron mass  $m^*$ , where  $k^2 = k_x^2 + k_y^2$ ,

and  $d = |\mathbf{d}|$  given by

$$d(\mathbf{r}, \mathbf{k}) = \sqrt{\lambda^2(ka)^2 + J^2 - 2\lambda J[k_y a \hat{m}_x(\mathbf{r}) - k_x a \hat{m}_y(\mathbf{r})]}. \quad (61)$$

Our analysis proceeds in three steps. (1) First, we analyze the real-space Berry curvature as a function of  $\lambda/J$ . Its integral

$$\mathcal{Q} = \frac{1}{2\pi} \int d^2r \Omega_{r_x r_y}, \quad \Omega_{r_x r_y} = \frac{1}{2d^3} \mathbf{d} \cdot (\partial_{r_x} \mathbf{d} \times \partial_{r_y} \mathbf{d}) \quad (62)$$

over a region with periodic boundary conditions is a Chern number, which is integer valued. However, when we analyze it in two different limits we get two different answers: we find that  $\mathcal{Q}$  vanishes in the strong SOC limit, while it is equal to the total skyrmion number of the spin texture for weak SOC (as we saw in the topological Hall effect analysis above). (2) Obviously this is only possible if the gap closes at a critical  $(\lambda/J)_c$  somewhere between these two limits. We explicitly show that this is indeed the case for a 2D skyrmion crystal. It follows that we must have  $\mathcal{Q}$  equal to the skyrmion number below  $(\lambda/J)_c$ , and zero above it. (3) Finally we investigate the momentum-space and mixed Berry curvatures as a function of  $\lambda/J$ . We find the mixed curvature can always be neglected in our semiclassical analysis, and the anomalous Hall response arising from the momentum space Berry curvature dominates in the strong SOC regime.

Using eq. (15), we write the real-space Berry curvature as the sum of two terms

$$\begin{aligned} \Omega_{r_x r_y} = & -\frac{J^3}{2d^3} \hat{\mathbf{m}}(\mathbf{r}) \cdot \partial_{r_x} \hat{\mathbf{m}}(\mathbf{r}) \times \partial_{r_y} \hat{\mathbf{m}}(\mathbf{r}) \\ & + \frac{\lambda J^2}{2d^3} (k_y a, -k_x a, 0) \cdot \partial_{r_x} \hat{\mathbf{m}}(\mathbf{r}) \times \partial_{r_y} \hat{\mathbf{m}}(\mathbf{r}). \end{aligned} \quad (63)$$

In the weak SOC limit  $d \approx J$ , the first term dominates and  $\Omega_{r_x r_y}$  is just the topological charge density. When integrated over a region with periodic boundary conditions, we see that  $\mathcal{Q}$  is the total skyrmion number. However, in the opposite limit of strong SOC,  $d \approx \lambda ka$ , the second term dominates, and  $\Omega_{r_x r_y}$  is *not* the topological charge density of the spin texture. We see that  $\Omega_{r_x r_y}$  scales like  $\sim (J/\lambda)^2 L_s^{-2} \ll L_s^{-2}$ , the scale of the real space Berry curvature for weak SOC.

We next show that  $\mathcal{Q}$  vanishes in the strong SOC limit. We see from (the second term of) eq. (63), with  $d = \lambda ka$ , that  $\Omega_{r_x r_y}$  is a function of both  $\mathbf{r}$  and  $\mathbf{k}$ . We focus on its  $\mathbf{r}$ -dependence at a fixed generic value of  $\mathbf{k}$ . In the spirit of the semiclassical transport calculations on the preceding sections, we set  $\mathbf{k} = \mathbf{k}_F$  on the Fermi surface. The spatial integral entering  $\mathcal{Q}$  is given by  $\mathcal{I} = \epsilon_{abc} \int dr_x \int dr_y \partial_{r_x} \hat{m}_a \partial_{r_y} \hat{m}_b$  over a region  $-L/2 \leq r_x < L/2$ ,  $-L/2 \leq r_y < L/2$  with periodic boundary conditions (PBCs):  $m_a(r_x, L/2) = m_a(r_x, -L/2)$  and  $m_a(L/2, r_y) = m_a(-L/2, r_y)$ . We first do an integration by parts in  $\int dr_y$  and then in  $\int dr_x$ . The boundary

terms vanish in both cases due to the PBCs. This effectively interchanges the  $r_x$  and  $r_y$  derivatives, and we obtain  $\mathcal{I} = \epsilon_{abc} \int dr_x \int dr_y \partial_{r_y} \hat{m}_a \partial_{r_x} \hat{m}_b$ . Interchanging the dummy indices  $a$  and  $b$ , we see that the integral vanishes and thus  $\mathcal{Q} = 0$  in the strong SOC limit.

To understand how the topological invariant  $\mathcal{Q}$  jumps from the non-zero skyrmion number in weak SOC to zero at strong SOC, we need to show that the gap closes at some intermediate value  $(\lambda/J)$ . For concreteness, let us analyze this question for a periodic skyrmion crystal (SkX) in 2D with skyrmion number one in each unit cell. The gap closes when  $d(\mathbf{r}, \mathbf{k}_F) = 0$  and the two bands  $\mathcal{E}_{\pm}$  become degenerate on the Fermi surface  $\mathbf{k}_F = k_F(\cos \theta, \sin \theta)$ . In order for this to occur all three components of  $\mathbf{d}$  in eq. (60) must vanish, so that

$$\lambda k_F a \sin \theta = J m_x(\mathbf{r}), \quad \lambda k_F a \cos \theta = -J m_y(\mathbf{r}), \quad m_z(\mathbf{r}) = 0. \quad (64)$$

The third equation  $m_z(\mathbf{r}^*) = 0$  defines a contour  $\mathbf{r} = \mathbf{r}^*$  in the SkX unit cell. Such a real space contour is guaranteed to exist for any texture with skyrmion number one. Adding the squares of the first two equations, and using  $m_x^2(\mathbf{r}^*) + m_y^2(\mathbf{r}^*) = 1$ , we find that the condition for gap closing is  $(\lambda/J)_c = 1/(k_F a) \sim O(1)$ .

To summarize, for the 2D skyrmion crystal we have found the critical value  $(\lambda/J)_c$  at which the gap closes on the Fermi surface, and  $d = 0$  implies that the real space Berry curvature becomes ill-defined. Since the Chern number  $\mathcal{Q}$  is a topological invariant, by continuity it must equal the skyrmion number for *all*  $(\lambda/J) < (\lambda/J)_c$ , even though we have explicitly shown this only in the weak SOC limit. Similarly,  $\mathcal{Q}$  vanishes for *all*  $(\lambda/J) > (\lambda/J)_c$ , even though we have computed this only in the strong SOC limit.

Since the real-space Berry curvature has vanishing impact in the strong SOC regime, we must investigate the effects of the other Berry curvatures in this regime. Computing the mixed Berry curvature  $\Omega_{r_x k_y}$  for the  $\mathbf{d}$ -vector of eq. (60), we see that it scales like  $(\lambda/J)(a/L_s) \ll 1$  for weak SOC and  $(J/\lambda)(a/L_s) \ll 1$  for strong SOC. Thus, in both limits, it is negligible compared to  $\mathbb{1}$  in eq. (13) in the semiclassical equations of motion.

Finally, we find that the momentum space Berry curvature for arbitrary  $\lambda/J$  is given by

$$\Omega_{k_x, k_y} = -\frac{1}{2d^3} J \lambda^2 a^2 m_z. \quad (65)$$

This expression reduces to the well-known result [4] for the  $\mathbf{k}$ -space Berry curvature for a uniform ferromagnet when we set  $\mathbf{m} = (0, 0, 1)$  independent of  $\mathbf{r}$ , and generalizes that result to an arbitrary spin texture. We see that  $\Omega_{k_x, k_y}$  scales like  $(\lambda/J)^2 a^2$  for weak SOC and as  $(J/\lambda) a^2$  for strong SOC. Therefore the momentum space Berry curvature is large in the strong SOC regime and the anomalous Hall effect will be the dominant contribution.

## X. CONCLUSIONS

The main results of our paper are already summarized in the Introduction. We conclude the paper with several open questions that could be addressed in future work. We have focused on solving the Boltzmann equation in the semiclassical regime  $k_F \sim a \ll \ell \ll L_s$ , where we derived the simple decomposition of eq. (3) in the weak SOC regime. The semiclassical approach, however, is equally valid for  $k_F \sim a \ll L_s \ll \ell$ . A unified treatment of phase space Berry curvatures in this limit is left for future work. One would need to treat the real-space Berry curvature in a manner analogous to the “strong field regime”  $\omega_c \tau \gg 1$  for external magnetic fields. It is well-known that the solution of the Boltzmann equation in such a regime is more involved than the one presented here, but it is certainly tractable.

We focused exclusively on the *intrinsic* anomalous Hall effect (AHE) that involves momentum-space Berry curvature, which is known in many materials to be the dominant contribution [2, 4]. However, there also exists *extrinsic* contributions to the AHE arising from skew and side jump scattering [2] in the presence of SOC scattering processes. Some progress in incorporating these effects in skyrmion materials has been reported in refs. [59, 60]. In principle, these effects can be included in the Boltzmann equation by going beyond the relaxation time approxima-

tion used above. The interplay between the topological Hall effect and the intrinsic and extrinsic AHEs is an interesting open question.

There are several important questions that go beyond the semiclassical Boltzmann approach. First, a semiclassical analysis becomes questionable when the skyrmion size becomes comparable to the lattice spacing  $a$ , and one must then resort to using the Kubo formula to compute conductivities. Some results along these lines were presented in ref. [30], but decomposing numerical results into anomalous and topological contributions is not straightforward. Second, the band index is a constant of motion in the semiclassical approach, which raises the question of how interband transitions affect the AHE and THE. Finally, note that the mixed (real/momentum space) Berry curvature  $\Omega_{r_i k_j}$  played no role in our final results because it scales like  $a/L_s$ , which is tiny in the semiclassical regime. It is an open question whether, outside this regime, there are observables for which the mixed space Berry curvature plays an important role.

**Acknowledgments:** We gratefully acknowledge support from the NSF Materials Research Science and Engineering Center Grant DMR-2011876. Z.A. was also supported by the Ohio State University President’s Postdoctoral Scholars Program.

- 
- [1] D. J. Thouless, M. Kohmoto, M. P. Nightingale, and M. den Nijs, Quantized hall conductance in a two-dimensional periodic potential, *Physical review letters* **49**, 405 (1982).
  - [2] N. Nagaosa, J. Sinova, S. Onoda, A. H. MacDonald, and N. P. Ong, Anomalous hall effect, *Reviews of modern physics* **82**, 1539 (2010).
  - [3] Y. Yao, L. Kleinman, A. MacDonald, J. Sinova, T. Jungwirth, D.-s. Wang, . f. E. Wang, and Q. Niu, First principles calculation of anomalous hall conductivity in ferromagnetic bcc fe, *Physical review letters* **92**, 037204 (2004).
  - [4] D. Xiao, M.-C. Chang, and Q. Niu, Berry phase effects on electronic properties, *Reviews of modern physics* **82**, 1959 (2010).
  - [5] F. Haldane, Berry curvature on the fermi surface: Anomalous hall effect as a topological fermi-liquid property, *Physical review letters* **93**, 206602 (2004).
  - [6] S. Onoda, N. Sugimoto, and N. Nagaosa, Intrinsic versus extrinsic anomalous hall effect in ferromagnets, *Physical review letters* **97**, 126602 (2006).
  - [7] N. Nagaosa and Y. Tokura, Topological properties and dynamics of magnetic skyrmions, *Nature nanotechnology* **8**, 899 (2013).
  - [8] M. Lee, W. Kang, Y. Onose, Y. Tokura, and N. P. Ong, Unusual Hall effect anomaly in MnSi under pressure, *Physical review letters* **102**, 186601 (2009).
  - [9] A. Neubauer, C. Pfleiderer, B. Binz, A. Rosch, R. Ritz, P. Niklowitz, and P. Böni, Topological Hall effect in the a phase of MnSi, *Physical review letters* **102**, 186602 (2009).
  - [10] N. Kanazawa, Y. Onose, T. Arima, D. Okuyama, K. Ohoyama, S. Wakimoto, K. Kakurai, S. Ishiwata, and Y. Tokura, Large topological Hall effect in a short-period helimagnet MnGe, *Physical review letters* **106**, 156603 (2011).
  - [11] Y. Li, N. Kanazawa, X. Yu, A. Tsukazaki, M. Kawasaki, M. Ichikawa, X. Jin, F. Kagawa, and Y. Tokura, Robust formation of skyrmions and topological Hall effect anomaly in epitaxial thin films of MnSi, *Physical review letters* **110**, 117202 (2013).
  - [12] J. Gallagher, K. Meng, J. Brangham, H. Wang, B. Esser, D. McComb, and F. Yang, Robust zero-field skyrmion formation in FeGe epitaxial thin films, *Physical review letters* **118**, 027201 (2017).
  - [13] A. S. Ahmed, J. Rowland, B. D. Esser, S. R. Dunsiger, D. W. McComb, M. Randeria, and R. K. Kawakami, Chiral bobbers and skyrmions in epitaxial FeGe/Si (111) films, *Physical Review Materials* **2**, 041401 (2018).
  - [14] A. S. Ahmed, A. J. Lee, N. Bagués, B. A. McCullian, A. M. Thabt, A. Perrine, P.-K. Wu, J. R. Rowland, M. Randeria, P. C. Hammel, *et al.*, Spin-Hall topological Hall effect in highly tunable Pt/ferrimagnetic-insulator bilayers, *Nano letters* **19**, 5683 (2019).
  - [15] Q. Shao, Y. Liu, G. Yu, S. K. Kim, X. Che, C. Tang, Q. L. He, Y. Tserkovnyak, J. Shi, and K. L. Wang, Topological Hall effect at above room temperature in heterostructures composed of a magnetic insulator and a heavy metal, *Nature Electronics* **2**, 182 (2019).
  - [16] J. Ye, Y. B. Kim, A. Millis, B. Shraiman, P. Majum-

- dar, and Z. Tešanović, Berry phase theory of the anomalous Hall effect: application to colossal magnetoresistance manganites, *Physical review letters* **83**, 3737 (1999).
- [17] P. Bruno, V. Dugaev, and M. Taillefumier, Topological Hall effect and Berry phase in magnetic nanostructures, *Physical review letters* **93**, 096806 (2004).
- [18] N. Nagaosa, X. Yu, and Y. Tokura, Gauge fields in real and momentum spaces in magnets: monopoles and skyrmions, *Philosophical Transactions of the Royal Society A: Mathematical, Physical and Engineering Sciences* **370**, 5806 (2012).
- [19] K.-W. Kim, H.-W. Lee, K.-J. Lee, and M. D. Stiles, Chirality from interfacial spin-orbit coupling effects in magnetic bilayers, *Physical review letters* **111**, 216601 (2013).
- [20] C. A. Akosa, H. Li, G. Tatara, and O. A. Tretiakov, Tuning the skyrmion Hall effect via engineering of spin-orbit interaction, *Physical Review Applied* **12**, 054032 (2019).
- [21] U. K. Roessler, A. Bogdanov, and C. Pfleiderer, Spontaneous skyrmion ground states in magnetic metals, *Nature* **442**, 797 (2006).
- [22] A. Fert, N. Reyren, and V. Cros, Magnetic skyrmions: advances in physics and potential applications, *Nature Reviews Materials* **2**, 1 (2017).
- [23] Y. Tokura and N. Kanazawa, Magnetic skyrmion materials, *Chemical Reviews* **121**, 2857 (2020).
- [24] Y. Shiomi, N. Kanazawa, K. Shibata, Y. Onose, and Y. Tokura, Topological Nernst effect in a three-dimensional skyrmion-lattice phase, *Physical Review B* **88**, 064409 (2013).
- [25] M. Hirschberger, L. Spitz, T. Nomoto, T. Kurumaji, S. Gao, J. Masell, T. Nakajima, A. Kikkawa, Y. Yamasaki, H. Sagayama, *et al.*, Topological Nernst effect of the two-dimensional skyrmion lattice, *Physical Review Letters* **125**, 076602 (2020).
- [26] K. K. Kolincio, M. Hirschberger, J. Masell, S. Gao, A. Kikkawa, Y. Taguchi, T.-h. Arima, N. Nagaosa, and Y. Tokura, Large Hall and Nernst responses from thermally induced spin chirality in a spin-trimer ferromagnet, *Proceedings of the National Academy of Sciences* **118**, e2023588118 (2021).
- [27] A. F. Scarioni, C. Barton, H. Corte-León, S. Sievers, X. Hu, F. Ajejas, W. Legrand, N. Reyren, V. Cros, O. Kazakova, *et al.*, Thermoelectric signature of individual skyrmions, *Physical Review Letters* **126**, 077202 (2021).
- [28] J. Macy, D. Ratkovski, P. P. Balakrishnan, M. Strungaru, Y.-C. Chiu, A. Flessa Savvidou, A. Moon, W. Zheng, A. Weiland, G. T. McCandless, *et al.*, Magnetic field-induced non-trivial electronic topology in  $\text{Fe}_{3-x}\text{GeTe}_2$ , *Applied Physics Reviews* **8**, 041401 (2021).
- [29] H. Zhang, C. Xu, and X. Ke, Topological Nernst effect, anomalous Nernst effect, and anomalous thermal Hall effect in the Dirac semimetal  $\text{Fe}_3\text{Sn}_2$ , *Physical Review B* **103**, L201101 (2021).
- [30] N. Verma, Z. Addison, and M. Randeria, Unified theory of the anomalous and topological Hall effects with phase-space Berry curvatures, *Science Advances* **8**, eabq2765 (2022).
- [31] Z. Addison, L. Keyes, and M. Randeria, Theory of topological nernst and thermoelectric transport in chiral magnets, *Phys. Rev. B* **108**, 014419 (2023).
- [32] G. Sundaram and Q. Niu, Wave-packet dynamics in slowly perturbed crystals: Gradient corrections and Berry-phase effects, *Physical Review B* **59**, 14915 (1999).
- [33] N. Cooper, B. Halperin, and I. Ruzin, Thermoelectric response of an interacting two-dimensional electron gas in a quantizing magnetic field, *Physical Review B* **55**, 2344 (1997).
- [34] J. Luttinger, Theory of thermal transport coefficients, *Physical Review* **135**, A1505 (1964).
- [35] T. Qin, Q. Niu, and J. Shi, Energy magnetization and the thermal hall effect, *Phys. Rev. Lett.* **107**, 236601 (2011).
- [36] S. Onoda, N. Sugimoto, and N. Nagaosa, Theory of non-equilibrium states driven by constant electromagnetic fields: —non-commutative quantum mechanics in the keldysh formalism—, *Progress of theoretical physics* **116**, 61 (2006).
- [37] N. Sugimoto, S. Onoda, and N. Nagaosa, Gauge covariant formulation of the wigner representation through deformation quantization: application to keldysh formalism with an electromagnetic field, *Progress of theoretical physics* **117**, 415 (2007).
- [38] A. Shitade, Heat transport as torsional responses and keldysh formalism in a curved spacetime, *Progress of Theoretical and Experimental Physics* **2014**, 123101 (2014).
- [39] A. Shitade, Theory of charge and heat polarizations with the keldysh formalism, *Journal of the Physical Society of Japan* **83**, 033708 (2014).
- [40] C. Xiao and Q. Niu, Unified bulk semiclassical theory for intrinsic thermal transport and magnetization currents, *Physical Review B* **101**, 235430 (2020).
- [41] Y. Fujishiro, N. Kanazawa, T. Nakajima, X. Yu, K. Ohishi, Y. Kawamura, K. Kakurai, T. Arima, H. Mitamura, A. Miyake, *et al.*, Topological transitions among skyrmion-and hedgehog-lattice states in cubic chiral magnets, *Nature communications* **10**, 1059 (2019).
- [42] D. Xiao, J. Shi, and Q. Niu, Berry phase correction to electron density of states in solids, *Physical review letters* **95**, 137204 (2005).
- [43] M. Nakahara, *Geometry, Topology and Physics* (Taylor and Francis, 2003).
- [44] A. Gromov and A. G. Abanov, Thermal hall effect and geometry with torsion, *Phys. Rev. Lett.* **114**, 016802 (2015).
- [45] Y. Zhang, Y. Gao, and D. Xiao, Thermodynamics of energy magnetization, *Phys. Rev. B* **102**, 235161 (2020).
- [46] E. Sondheimer, The theory of the galvanomagnetic and thermomagnetic effects in metals, *Proceedings of the Royal Society of London. Series A. Mathematical and Physical Sciences* **193**, 484 (1948).
- [47] Y. Cui, Z. Li, H. Chen, Y. Wu, Y. Chen, K. Pei, T. Wu, N. Xie, R. Che, X. Qiu, *et al.*, Antisymmetric planar hall effect in rutile oxide films induced by the lorentz force, *Science Bulletin* (2024).
- [48] Y. You, Y. Gong, H. Li, Z. Li, M. Zhu, J. Tang, E. Liu, Y. Yao, G. Xu, F. Xu, *et al.*, Angular dependence of the topological hall effect in the uniaxial van der waals ferromagnet  $\text{Fe}_3\text{GeTe}_2$ , *Physical Review B* **100**, 134441 (2019).
- [49] Y. Wang, J. Yan, J. Li, S. Wang, M. Song, J. Song, Z. Li, K. Chen, Y. Qin, L. Ling, *et al.*, Magnetic anisotropy and topological hall effect in the trigonal chromium tellurides  $\text{Cr}_5\text{Te}_8$ , *Physical Review B* **100**, 024434 (2019).
- [50] J. Ge, D. Ma, Y. Liu, H. Wang, Y. Li, J. Luo, T. Luo, Y. Xing, J. Yan, D. Mandrus, *et al.*, Unconventional hall effect induced by berry curvature, *National science re-*

- view **7**, 1879 (2020).
- [51] H. Tan, Y. Liu, and B. Yan, Unconventional anomalous hall effect from magnetization parallel to the electric field, *Physical Review B* **103**, 214438 (2021).
  - [52] J. Zhou, W. Zhang, Y.-C. Lin, J. Cao, Y. Zhou, W. Jiang, H. Du, B. Tang, J. Shi, B. Jiang, *et al.*, Heterodimensional superlattice with in-plane anomalous hall effect, *Nature* **609**, 46 (2022).
  - [53] Y. Chen, Y. Zhu, R. Lin, W. Niu, R. Liu, W. Zhuang, X. Zhang, J. Liang, W. Sun, Z. Chen, *et al.*, Observation of colossal topological hall effect in noncoplanar ferromagnet  $\text{Cr}_5\text{Te}_6$  thin films, *Advanced Functional Materials* **33**, 2302984 (2023).
  - [54] J. Cao, W. Jiang, X.-P. Li, D. Tu, J. Zhou, J. Zhou, and Y. Yao, In-plane anomalous hall effect in pt-symmetric antiferromagnetic materials, *Physical Review Letters* **130**, 166702 (2023).
  - [55] T. Yokouchi, N. Kanazawa, A. Tsukazaki, Y. Kozuka, A. Kikkawa, Y. Taguchi, M. Kawasaki, M. Ichikawa, F. Kagawa, and Y. Tokura, Formation of in-plane skyrmions in epitaxial  $\text{MnSi}$  thin films as revealed by planar hall effect, *Journal of the Physical Society of Japan* **84**, 104708 (2015).
  - [56] N. Kanazawa, S. Seki, and Y. Tokura, Noncentrosymmetric magnets hosting magnetic skyrmions, *Advanced Materials* **29**, 1603227 (2017).
  - [57] D. Wolf, S. Schneider, U. K. Rößler, A. Kovács, M. Schmidt, R. E. Dunin-Borkowski, B. Büchner, B. Rellinghaus, and A. Lubk, Unveiling the three-dimensional magnetic texture of skyrmion tubes, *Nature nanotechnology* **17**, 250 (2022).
  - [58] T. Kurumaji, Symmetry-based requirement for the measurement of electrical and thermal hall conductivity under an in-plane magnetic field, *Phys. Rev. Res.* **5**, 023138 (2023).
  - [59] F. R. Lux, F. Freimuth, S. Blügel, and Y. Mokrousov, Chiral hall effect in noncollinear magnets from a cyclic cohomology approach, *Physical review letters* **124**, 096602 (2020).
  - [60] J. Bouaziz, H. Ishida, S. Lounis, and S. Blügel, Transverse transport in two-dimensional relativistic systems with nontrivial spin textures, *Physical review letters* **126**, 147203 (2021).



## Appendix A: Semiclassical Equations of Motion

We briefly describe the semiclassical framework. A detailed description of this procedure can be found in Appendix A of Ref. [31] and in Refs. [4, 32]. The standard semiclassical procedure starts by expanding the Hamiltonian (4) in powers of  $(\hat{\mathbf{r}} - \mathbf{r}_c)$  with  $\mathbf{r}_c$  being some arbitrary real space point. Because the magnetic texture varies on the scale of  $L_s$ , spatial derivatives scale like  $\nabla_{\mathbf{r}} \sim 1/L_s$ . The other length scale in the system is the lattice spacing  $a$  which we take to satisfy  $a/L_s \ll 1$ . For computing transport coefficients it is sufficient to keep just the leading order correction, so that  $\hat{H} \approx \hat{H}_c + \Delta\hat{H}$ , where  $\hat{H}_c(\mathbf{r}_c) = \hat{H}(\hat{\mathbf{r}} \rightarrow \mathbf{r}_c)$ , and

$$\Delta\hat{H}(\mathbf{r}_c) = -J \sum_{i,\sigma\sigma'} \hat{c}_{i\sigma}^\dagger \left( (\mathbf{r}_i - \mathbf{r}_c) \cdot \nabla_{\mathbf{r}_c} \hat{\mathbf{m}}(\mathbf{r}_c) \cdot \boldsymbol{\sigma}^{\sigma\sigma'} \right) \hat{c}_{i\sigma'}. \quad (\text{A1})$$

The contribution to the Hamiltonian  $\hat{H}_c$  has discrete translational symmetry and thus is able to be written in the Bloch basis with states labeled by crystal momentum  $\mathbf{q}$ . The associated Bloch Hamiltonian is  $\hat{H}_{sc}(\mathbf{r}_c, \mathbf{q}) = \varepsilon(\mathbf{q})\mathbb{1} + \mathbf{d}(\mathbf{r}_c, \mathbf{q}) \cdot \boldsymbol{\sigma}$ , where  $\mathbf{d}(\mathbf{r}_c, \mathbf{q})$  is given by Eq. (9). The Hamiltonian  $\hat{H}_c$  has eigenstates  $|\psi_{\pm}(\mathbf{r}_c, \mathbf{q})\rangle$ , whose lattice periodic part we denote as  $|u_{\pm}(\mathbf{r}_c, \mathbf{q})\rangle$ , and with energy eigenvalues  $\mathcal{E}_{\pm}(\mathbf{r}_c, \mathbf{q}) = \varepsilon(\mathbf{q}) \pm |\mathbf{d}(\mathbf{r}_c, \mathbf{q})|$ , where  $\pm$  labels the two bands.

Wavepackets  $|W_{\pm}(\mathbf{r}_c, \mathbf{q}_c)\rangle = \int d\mathbf{q} \gamma_{\pm}(\mathbf{r}_c, \mathbf{q}, t) |\psi_{\pm}(\mathbf{r}_c, \mathbf{q})\rangle$  are constructed from the Bloch states  $|\psi_{\pm}(\mathbf{r}_c, \mathbf{q})\rangle$  with envelope functions  $\gamma_{\pm}(\mathbf{r}_c, \mathbf{q})$  such that the wavepackets are centered at  $(\mathbf{r}_c, \mathbf{q}_c)$ . In the semiclassical approach, the band index is a good quantum number and there are no interband transitions. To incorporate electromagnetic perturbations, the Hamiltonian in eq. (4) is modified by addition of a scalar potential  $-e\phi(\hat{\mathbf{r}}, t)$  and incorporation of a gauge invariant momentum,  $\mathbf{k}_c \equiv \mathbf{q}_c + e\mathbf{A}$ , where  $e$  is the positive electron charge and  $\mathbf{A}$  is the vector potential. The wavepacket energies with the scalar potential are to first order

$$\langle W_{\pm} | \hat{H} | W_{\pm} \rangle \approx \tilde{\mathcal{E}}_{\pm}(\mathbf{r}_c, \mathbf{k}_c) - e\phi(\mathbf{r}_c, t) = \mathcal{E}_{\pm}(\mathbf{r}_c, \mathbf{k}_c) + \langle W_{\pm} | \Delta\hat{H} | W_{\pm} \rangle - e\phi(\mathbf{r}_c, t) \quad (\text{A2})$$

In this case, the energetic correction  $\Delta\mathcal{E} = \langle W_{\pm} | \Delta\hat{H} | W_{\pm} \rangle$  is the orbital magnetization energy of the wavepacket.

Following the discussion of Ref. [4], the expectation value of an operator is

$$\mathcal{O} = \int_{\boldsymbol{\xi}} \mathcal{D}(\boldsymbol{\xi}) f(\boldsymbol{\xi}) \langle W(\boldsymbol{\xi}) | \hat{\mathcal{O}} \delta(\mathbf{r} - \hat{\mathbf{r}}) | W(\boldsymbol{\xi}) \rangle. \quad (\text{A3})$$

By expanding  $\delta(\hat{\mathbf{r}} - \mathbf{r}_c)$  to first order, the expectation value of the operator consists of the operator evaluated at  $\mathbf{r}_c$  and a dipole correction [4], as seen in Eq. (32), where the dipole correction takes the form of the orbital magnetization.

For simplicity, we drop the "c" label on the coordinates and define the phase-space vector  $\boldsymbol{\xi} \equiv (r_x, r_y, r_z, k_x, k_y, k_z)$ . Starting with the semiclassical Lagrangian

$$L_{\pm}(\boldsymbol{\xi}) = \langle W_{\pm}(\boldsymbol{\xi}) | i\hbar \frac{d}{dt} - \hat{H} | W_{\pm}(\boldsymbol{\xi}) \rangle. \quad (\text{A4})$$

we can arrive at the equations of motion of  $\boldsymbol{\xi}$

$$\sum_{\beta} \Gamma_{\alpha\beta}^{\pm}(\boldsymbol{\xi}) \dot{\xi}_{\beta} = \frac{1}{\hbar} \nabla_{\xi_{\alpha}} (\tilde{\mathcal{E}}_{\pm}(\boldsymbol{\xi}) - e\phi(\mathbf{r}, t)) \quad (\text{A5})$$

using the methodology of Ref. [32]. Here

$$\tilde{\Gamma}^{\pm}(\boldsymbol{\xi}) = \begin{pmatrix} 0 & \Omega_{r_x r_y}^{\pm} - \frac{e}{\hbar} F_{xy} & \Omega_{r_x r_z}^{\pm} + \frac{e}{\hbar} F_{zx} & \Omega_{r_x k_x}^{\pm} - 1 & \Omega_{r_x k_y}^{\pm} & \Omega_{r_x k_z}^{\pm} \\ -\Omega_{r_x r_y}^{\pm} + \frac{e}{\hbar} F_{xy} & 0 & \Omega_{r_y r_z}^{\pm} - \frac{e}{\hbar} F_{yz} & \Omega_{r_y k_x}^{\pm} & \Omega_{r_y k_y}^{\pm} - 1 & \Omega_{r_y k_z}^{\pm} \\ -\Omega_{r_x r_z}^{\pm} - \frac{e}{\hbar} F_{zx} & -\Omega_{r_y r_z}^{\pm} + \frac{e}{\hbar} F_{yz} & 0 & \Omega_{r_z k_x}^{\pm} & \Omega_{r_z k_y}^{\pm} & \Omega_{r_z k_z}^{\pm} - 1 \\ -\Omega_{r_x k_x}^{\pm} + 1 & -\Omega_{r_y k_x}^{\pm} & -\Omega_{r_z k_x}^{\pm} & 0 & \Omega_{k_x k_y}^{\pm} & \Omega_{k_x k_z}^{\pm} \\ -\Omega_{r_x k_y}^{\pm} & -\Omega_{r_y k_y}^{\pm} + 1 & -\Omega_{r_z k_y}^{\pm} & -\Omega_{k_x k_y}^{\pm} & 0 & \Omega_{k_y k_z}^{\pm} \\ -\Omega_{r_x k_z}^{\pm} & -\Omega_{r_y k_z}^{\pm} & -\Omega_{r_z k_z}^{\pm} + 1 & -\Omega_{k_x k_z}^{\pm} & -\Omega_{k_y k_z}^{\pm} & 0 \end{pmatrix} \quad (\text{A6})$$

The phase space Berry curvatures  $\Omega_{\xi_\alpha \xi_\beta}^\pm = \partial_{\xi_\alpha} \mathcal{A}_{\xi_\beta}^\pm - \partial_{\xi_\beta} \mathcal{A}_{\xi_\alpha}^\pm$ , defined in terms of the Berry connection  $\mathcal{A}_{\xi_\alpha}^\pm = i \langle u_\pm(\boldsymbol{\xi}) | \partial_{\xi_\alpha} | u_\pm(\boldsymbol{\xi}) \rangle$ , can be written more conveniently as

$$\Omega_{\xi_\alpha \xi_\beta}^\pm(\boldsymbol{\xi}) = \pm \frac{1}{2} \hat{\mathbf{d}} \cdot (\partial_{\xi_\alpha} \hat{\mathbf{d}} \times \partial_{\xi_\beta} \hat{\mathbf{d}}), \quad (\text{A7})$$

The magnetic field is defined via the electromagnetic field tensor

$$F_{ij} = \partial_{r_i} A_j - \partial_{r_j} A_i. \quad (\text{A8})$$

We have used script  $\mathcal{A}$  to denote Berry connection and text  $\mathbf{A}$  to denote electromagnetic vector potential. Moving forward, we will omit writing the band index unless necessary. In order to isolate the equations of motion,  $\dot{\mathbf{r}}_c$  and  $\dot{\mathbf{k}}_c$ , we must invert  $\overleftrightarrow{\Gamma}$ . The inverse matrix  $\overleftrightarrow{\Gamma}^{-1}$  can be written in block form

$$\overleftrightarrow{\Gamma}^{-1}(\boldsymbol{\xi}) = \frac{1}{\mathcal{D}(\boldsymbol{\xi})} \begin{pmatrix} \overleftrightarrow{\mathbf{K}}(\boldsymbol{\xi}) & \overleftrightarrow{\mathbf{S}}(\boldsymbol{\xi}) \\ -\overleftrightarrow{\mathbf{S}}^T(\boldsymbol{\xi}) & \overleftrightarrow{\mathbf{R}}(\boldsymbol{\xi}) \end{pmatrix} \quad (\text{A9})$$

where

$$\begin{aligned} \mathbf{K}_{ij}(\boldsymbol{\xi}) &= \Omega_{k_i k_j} - \sum_l (\Omega_{k_i k_j} \Omega_{r_l k_l} + \Omega_{k_j k_l} \Omega_{r_l k_i} - \Omega_{k_i k_l} \Omega_{r_l k_j}) |\epsilon_{ijl}| \\ \mathbf{R}_{ij}(\boldsymbol{\xi}) &= (\Omega_{r_i r_j} - \frac{e}{\hbar} F_{ij}) - \sum_l \left( (\Omega_{r_i r_j} - \frac{e}{\hbar} F_{ij}) \Omega_{r_l k_l} + (\Omega_{r_j r_l} - \frac{e}{\hbar} F_{jl}) \Omega_{r_i k_l} - (\Omega_{r_i r_l} - \frac{e}{\hbar} F_{il}) \Omega_{r_j k_l} \right) |\epsilon_{ijl}| \\ \mathbf{S}_{ij}(\boldsymbol{\xi}) &= (1 - \sum_l \Omega_{r_l k_l}) \delta_{ij} + \Omega_{r_j k_i} - \frac{1}{2} \delta_{ij} \sum_{nm} |\epsilon_{inm}| \left( \Omega_{k_n k_m} (\Omega_{r_n r_m} - \frac{e}{\hbar} F_{nm}) - \Omega_{r_n k_n} \Omega_{r_m k_m} + \Omega_{r_n k_m} \Omega_{r_m k_n} \right) \\ &\quad + \sum_l |\epsilon_{ijl}| \left( \Omega_{k_i k_l} (\Omega_{r_j r_l} - \frac{e}{\hbar} F_{jl}) + \Omega_{r_j k_l} \Omega_{r_l k_i} - \Omega_{r_j k_i} \Omega_{r_l k_l} \right) \\ \mathcal{D}(\boldsymbol{\xi}) &= \text{pf}(\Gamma(\boldsymbol{\xi})) = \left| 1 - \sum_i \Omega_{r_i k_i} + \frac{1}{2} \sum_{i,j} (1 - \delta_{ij}) \left( \Omega_{r_i k_i} \Omega_{r_j k_j} - (\Omega_{r_i r_j} - \frac{e}{\hbar} F_{ij}) \Omega_{k_i k_j} - \Omega_{r_i k_j} \Omega_{r_j k_i} \right) \right. \\ &\quad \left. + \sum_{ijk, \alpha\beta\gamma} \epsilon_{ijk} \epsilon_{\alpha\beta\gamma} \left( \frac{1}{4} \Omega_{k_\alpha k_\beta} (\Omega_{r_i r_j} - \frac{e}{\hbar} F_{ij}) \Omega_{r_k k_\gamma} - \frac{1}{6} \Omega_{r_i k_\alpha} \Omega_{r_j k_\beta} \Omega_{r_k k_\gamma} \right) \right| \end{aligned} \quad (\text{A10})$$

where  $i, j, k, l \in \{x, y, z\}$ .  $\overleftrightarrow{\mathbf{K}}$ ,  $\overleftrightarrow{\mathbf{R}}$ , and  $\overleftrightarrow{\mathbf{S}}$  are each  $3 \times 3$  matrices, and thus  $\overleftrightarrow{\Gamma}^{-1}$  is  $6 \times 6$ .

The notation  $|\epsilon_{ijk}|$  serves to enforce that  $i \neq j \neq k$ . Note the placement of indices explicitly in r-space and k-space in the above expressions. Terms like  $\Omega_{r_i r_i}$  vanish automatically due to the antisymmetry of the Berry curvature, but a term like  $\Omega_{r_i k_i}$  doesn't necessarily vanish. This is why we include the notation  $|\epsilon_{ijk}|$  where appropriate.

For either  $J \ll \lambda$  or  $J \gg \lambda$  the leading order contribution to the Berry curvatures are small quantities. For example in the regime  $\lambda \ll J$

$$\begin{aligned} \Omega_{k_\alpha k_\beta} &\sim a^2 (\lambda/J)^2 \\ \Omega_{r_\alpha k_\beta} &\sim (a/L_s) (\lambda/J) \\ \Omega_{r_\alpha r_\beta} &\sim 1/L_s^2. \end{aligned} \quad (\text{A11})$$

where we note that  $L_s$  is the largest length scale in the problem. We therefore see that the largest part of each of these block matrices is the term with the lowest power of Berry curvatures. Thus,  $\mathbf{K}_{ij} \approx \Omega_{k_i k_j}$ ,  $\mathbf{R}_{ij} \approx \Omega_{r_i r_j} - \frac{e}{\hbar} F_{ij}$ , and  $\mathbf{S}_{ij} \approx \delta_{ij}$ .

We end this Appendix by comments on why we write  $\overleftrightarrow{\Gamma}^{-1}$  in the form shown in eqs. (16) and (A9) with the pfaffian  $\mathcal{D} = \text{pf} \Gamma$  factored out. The usual expression for the inverse of a matrix  $\overleftrightarrow{\Gamma}^{-1} = (1/\det \overleftrightarrow{\Gamma}) \text{adj} \overleftrightarrow{\Gamma}$  is in terms of the adjugate of the matrix divided by the determinant, rather than involving the pfaffian. We already explained in the main text that the expression we use makes transparent the cancellation with the same pfaffian that appears in the phase space volume.

We now show why this expression is quite natural for the inverse of any  $2n \times 2n$  real antisymmetric matrix  $\overleftrightarrow{\Gamma}$ . While we cannot diagonalize  $\overleftrightarrow{\Gamma}$  with a real matrix, using a suitable orthogonal matrix  $\overleftrightarrow{Q}$  we can write its as

$$\overleftrightarrow{\Gamma} = \overleftrightarrow{Q} \overleftrightarrow{\Lambda} \overleftrightarrow{Q}^T \quad (\text{A12})$$

where  $\overleftrightarrow{\Lambda}$  is block diagonal:

$$\overleftrightarrow{\Lambda} = \begin{pmatrix} 0 & \lambda_1 & & \dots & & 0 \\ -\lambda_1 & 0 & & & & \\ & & 0 & \lambda_2 & & \\ & & -\lambda_2 & 0 & & \\ \vdots & & & & \ddots & \vdots \\ & & & & & 0 & \lambda_n \\ 0 & & & \dots & -\lambda_n & 0 \end{pmatrix} \quad (\text{A13})$$

Its pfaffian is  $\Lambda = \lambda_1 \lambda_2 \dots \lambda_n$ , and the inverse of  $\overleftrightarrow{\Lambda}$  is given by

$$\overleftrightarrow{\Lambda}^{-1} = \begin{pmatrix} 0 & -1/\lambda_1 & \dots & & & 0 \\ 1/\lambda_1 & 0 & & & & \\ \vdots & & \ddots & & & \vdots \\ & & & 0 & -1/\lambda_n & \\ 0 & \dots & 1/\lambda_n & 0 & & \end{pmatrix} = \frac{1}{\lambda_1 \lambda_2 \dots \lambda_n} \begin{pmatrix} 0 & -\lambda_2 \dots \lambda_n & \dots & & & 0 \\ \lambda_2 \dots \lambda_n & 0 & & & & \\ \vdots & & \ddots & & & \vdots \\ & & & 0 & -\lambda_1 \dots \lambda_{n-1} & \\ 0 & \dots & \lambda_1 \dots \lambda_{n-1} & 0 & & \end{pmatrix} \quad (\text{A14})$$

Because  $\overleftrightarrow{Q}$  is orthogonal, we have  $\text{pf} \Gamma = \text{pf} \Lambda$  and  $\overleftrightarrow{\Gamma}^{-1} = \overleftrightarrow{Q} \overleftrightarrow{\Lambda}^{-1} \overleftrightarrow{Q}^\top$ .

## Appendix B: Derivation of Phase Space Measure

Liouville's theorem states that the phase-space distribution function must remain constant along phase-space trajectories such that the phase-space volume

$$\mathcal{V} = \mathcal{C}(\boldsymbol{\xi}) dr_x \wedge dr_y \wedge dr_z \wedge dk_x \wedge dk_y \wedge dk_z \quad (\text{B1})$$

remains invariant under time evolution; i.e., the Lie derivative with respect to the velocity field  $\dot{\boldsymbol{\xi}}$  vanishes:  $\mathcal{L}_{\dot{\boldsymbol{\xi}}} \mathcal{V} = 0$ . The velocity field is defined

$$\dot{\boldsymbol{\xi}} = \frac{d\xi_i}{dt} \frac{\partial}{\partial \xi^i} \equiv \frac{d}{dt}. \quad (\text{B2})$$

We will employ the notation  $\mathcal{L}_t \equiv \mathcal{L}_{\dot{\boldsymbol{\xi}}}$  to elude to the fact that the change of the volume form along the flow of  $\dot{\boldsymbol{\xi}}$  measures the change of the volume form in time.

In the absence of phase-space curvatures,  $\mathbf{k}$  and  $\mathbf{r}$  are conjugate variables that satisfy the canonical Poisson bracket relations:  $\{r_i, k_j\} = \delta_{ij}$  such that Liouville's theorem is trivially satisfied ( $\mathcal{L}_t \mathcal{V} = 0$ ) with  $\mathcal{C}(\boldsymbol{\xi}) = 1$ . However, in the presence of phase space curvatures,  $\mathbf{k}$  and  $\mathbf{r}$  are no longer conjugate variables ( $\{r_i, k_j\} \neq \delta_{ij}$ ) and thus, in order to satisfy Liouville's theorem, the phase-space measure must be altered.

Our strategy to compute  $\mathcal{C}(\boldsymbol{\xi})$  in terms of phase-space curvatures is to propose the solution  $\mathcal{C}(\boldsymbol{\xi}) = \mathcal{D}(\boldsymbol{\xi}) = \sqrt{\det(\overleftrightarrow{\Gamma})}$  and then prove that it satisfies the constraint  $\mathcal{L}_t \mathcal{V} = 0$ . We define the two-form  $\omega = \sum_{ij} \Gamma_{ij} d\xi_i \wedge d\xi_j / 2$  and relate it

to  $\mathcal{V}$  by noting that

$$\begin{aligned} \frac{\omega \wedge \omega \wedge \omega}{6} &= \frac{1}{2^3 3!} \Gamma_{ij} \Gamma_{lk} \Gamma_{nm} d\xi_i \wedge d\xi_j \wedge d\xi_l \wedge d\xi_k \wedge d\xi_n \wedge d\xi_m \\ &= \sqrt{\det(\overline{\Gamma})} dr_x \wedge dr_y \wedge dr_z \wedge dk_x \wedge dk_y \wedge dk_z \\ &= \mathcal{V}. \end{aligned} \quad (\text{B3})$$

This relation leads to the Lie derivative being  $\mathcal{L}_t \mathcal{V} = \omega \wedge \omega \wedge \mathcal{L}_t \omega$ . We next use the Cartan formula to rewrite the Lie derivative on  $\omega$

$$\mathcal{L}_t \omega = i_t(d\omega) + d(i_t \omega) \quad (\text{B4})$$

where  $d$  is the exterior derivative and  $i_t$  is the interior product [43]. To prove that  $\mathcal{L}_t(V)$  vanishes, we first note that

$$\begin{aligned} d(i_t \omega) &= \frac{1}{2} \sum_{ij} d(\Gamma_{ij} \dot{\xi}_i d\xi_j - \Gamma_{ij} \dot{\xi}_j d\xi_i) = \sum_{ij} d(\Gamma_{ij} \dot{\xi}_i d\xi_j) \\ &= - \sum_i \frac{1}{\hbar} d\left(\partial_{\xi_i}(\varepsilon(\boldsymbol{\xi}) - e\phi(\mathbf{r}))\right) d\xi_i \\ &= - \sum_{ij} \frac{1}{\hbar} \partial_{\xi_j} \partial_{\xi_i}(\varepsilon(\boldsymbol{\xi}) - e\phi(\mathbf{r})) d\xi_j \wedge d\xi_i \end{aligned} \quad (\text{B5})$$

which vanishes as it is a product of a symmetric and an anti-symmetric tensor in  $i, j$ . Secondly, we may write  $\omega = d\eta$  with

$$\eta = \sum_i (\mathcal{A}_{\xi_i} + P_i) d\xi_i \quad (\text{B6})$$

where  $\mathcal{A}_i$  are the Berry connections and  $\mathbf{P} = (-k_x, -k_y, -k_z, r_x, r_y, r_z)/2$  such that  $d\omega = d^2\eta = 0$ . We have shown that  $d(i_t \omega) = 0$  and  $d\omega = 0$  so that by Eq. (20),  $\mathcal{L}_t \omega = 0$  and hence,  $\mathcal{L}_t \mathcal{V} = 0$ . This fixes the measure up to an overall constant that can be determined by noting that in the absence of curvatures,  $\mathcal{D}(\boldsymbol{\xi}) = 1$ .

### Appendix C: Solution to Boltzmann Equation

There are two driving fields present in the problem,  $\mathbf{E} - 1/e \nabla_r \mu$  and  $-\nabla_r T$ . We write the distribution function as

$$f^\pm(\boldsymbol{\xi}) = f_{\text{leq}}^\pm(\boldsymbol{\xi}) + \delta f^\pm(\boldsymbol{\xi}), \quad (\text{C1})$$

where  $\delta f^\pm(\boldsymbol{\xi})$  represents deviations from local equilibrium. From now on, we will omit writing the band index and  $\boldsymbol{\xi}$  argument, unless necessary. Which wish to solve for  $\delta f$  in the regime of linear response, so we shall drop any terms which are higher order in electric field, chemical potential gradient, or temperature gradient.

Thus the Boltzmann equation in the relaxation time approximation can be written as

$$-\frac{\delta f}{\tau} = \nabla_k (f_{\text{leq}} + \delta f) \cdot \dot{\mathbf{k}} + \nabla_r (f_{\text{leq}} + \delta f) \cdot \dot{\mathbf{r}}. \quad (\text{C2})$$

Analyzing spatial gradient term  $\nabla_r (f_{\text{leq}} + \delta f)$ :

$$\nabla_r (f_{\text{leq}} + \delta f) = \nabla_r \tilde{\mathcal{E}} \partial_{\tilde{\mathcal{E}}} (f_{\text{leq}} + \delta f) + \nabla_r T \partial_T (f_{\text{leq}} + \delta f) + \nabla_r \mu \partial_\mu (f_{\text{leq}} + \delta f). \quad (\text{C3})$$

The terms  $\nabla_r T \partial_T (\delta f)$  and  $\nabla_r \mu \partial_\mu (\delta f)$  are higher order and shall be dropped. Thus, to linear order in the driving fields, we have

$$-\frac{\delta f}{\tau} = \nabla_k f_{\text{eq}} \cdot \dot{\mathbf{k}}^{(1)} + \nabla_k (\delta f) \cdot \dot{\mathbf{k}}^{(0)} + \nabla_r \tilde{\mathcal{E}} \partial_{\tilde{\mathcal{E}}} f_{\text{eq}} \cdot \dot{\mathbf{r}}^{(1)} + \nabla_r T \partial_T f_{\text{eq}} \cdot \dot{\mathbf{r}}^{(0)} + \nabla_r \mu \partial_\mu f_{\text{eq}} \cdot \dot{\mathbf{r}}^{(0)} + \nabla_r \tilde{\mathcal{E}} \partial_{\tilde{\mathcal{E}}} (\delta f) \cdot \dot{\mathbf{r}}^{(0)}, \quad (\text{C4})$$

where  $\dot{\mathbf{r}}^{(0)}$  and  $\dot{\mathbf{k}}^{(0)}$  indicate the equations of motion to 0th order in  $\mathbf{E}$ , and,  $\dot{\mathbf{r}}^{(1)}$  and  $\dot{\mathbf{k}}^{(1)}$  are to first order in  $\mathbf{E}$ , and where we have replaced  $f_{\text{leq}}(\boldsymbol{\xi})$  with  $f_{\text{eq}}(\mathbf{k})$  as we only consider small perturbation of the fields about a homogeneous

background. For example, we consider  $\mu(\mathbf{r}) \approx \mu_0 + \nabla_r \mu$ , which to leading order in gradients allows us to neglect the dependence in  $f_{\text{ieq}}(\boldsymbol{\xi})$  of  $\nabla_r \mu$ . We collect all  $\delta f$  terms:

$$\left(1 + \tau(\dot{\mathbf{k}}^{(0)} \cdot \nabla_k + \dot{\mathbf{r}}^{(0)} \cdot \nabla_r \tilde{\mathcal{E}} \partial_{\tilde{\mathcal{E}}})\right) \delta f = -\tau \left( (\dot{\mathbf{k}}^{(1)} \cdot \nabla_k \tilde{\mathcal{E}} + \dot{\mathbf{r}}^{(1)} \cdot \nabla_r \tilde{\mathcal{E}} + \dot{\mathbf{r}}^{(0)} \cdot \nabla_r \mu) \partial_{\tilde{\mathcal{E}}} + \dot{\mathbf{r}}^{(0)} \cdot \nabla_r T \partial_T \right) f_{\text{ieq}} \quad (\text{C5})$$

Next we define the operator  $1 + \mathbb{P} \equiv 1 + \tau(\dot{\mathbf{k}}^{(0)} \cdot \nabla_k + \dot{\mathbf{r}}^{(0)} \cdot \nabla_r \tilde{\mathcal{E}} \partial_{\tilde{\mathcal{E}}})$ . To first order in driving fields we find

$$\delta f = -\tau(1 + \mathbb{P})^{-1} \left( (\dot{\mathbf{k}}^{(1)} \cdot \nabla_k \tilde{\mathcal{E}} + \dot{\mathbf{r}}^{(1)} \cdot \nabla_r \tilde{\mathcal{E}} + \dot{\mathbf{r}}^{(0)} \cdot \nabla_r \mu) \partial_{\tilde{\mathcal{E}}} + \dot{\mathbf{r}}^{(0)} \cdot \nabla_r T \partial_T \right) f_{\text{ieq}}. \quad (\text{C6})$$

**Solution to Boltzmann Equation in the Small SOC Regime:** We now simplify this linear response expression by considering the regime  $\lambda \ll J \ll t$  and  $a \ll \ell \ll L_s$ . Recall that the energy corrections  $\Delta \mathcal{E}$  are smaller than  $\mathcal{E}$  by a factor of  $a/L_s$ , so we approximate  $\tilde{\mathcal{E}}(\boldsymbol{\xi}) \approx \mathcal{E}(\boldsymbol{\xi})$ . It will also be useful to keep in mind the expansion of  $\mathcal{E}(\boldsymbol{\xi})$  in powers of  $\lambda$ :

$$\mathcal{E}_{\pm}(\boldsymbol{\xi}) \approx \varepsilon_{\pm}(\mathbf{k}) \pm \frac{\lambda}{at} \hat{m}_i(\mathbf{r}) \chi_{ji} \partial_{k_j} \varepsilon + \mathcal{O}(\lambda^2) \quad (\text{C7})$$

where  $\varepsilon_{\pm}(\mathbf{k}) = \varepsilon(\mathbf{k}) \pm J$ . This expansion shows that  $\nabla_r \mathcal{E} \sim \lambda/L_s$ . Similarly using the scaling relations in Eq. (A11) we see that  $\dot{\mathbf{k}}^{(1)} \cdot \nabla_k \mathcal{E} \ll \dot{\mathbf{r}}^{(1)} \cdot \nabla_r \mathcal{E}$ . The operator  $\mathbb{P}$  appears in combination with the derivatives  $\partial_T f_{\text{ieq}}$  and  $\partial_{\mathcal{E}} f_{\text{ieq}}$ . At temperatures much less than the Fermi temperature, these functions are peaked in a region  $k_B T$  around the Fermi energy, and so we take  $(1/\hbar) \nabla_k \mathcal{E} \sim v_F$ . Again using the scaling relations in Eq. (A11) and the scaling  $\nabla_r \sim (1/L_s)$  and  $\nabla_k \sim a$ , and keeping in mind that  $v_F \tau = \ell$ , we find that the leading order contribution to the operator  $\mathbb{P}$  is at most of order  $\ell/L_s$ . This allows us to make the approximation  $(1 + \mathbb{P})^{-1} \approx (1 - \mathbb{P})$ . This analysis leads determines the leading order contribution to  $\delta f$  that we may write as

$$\delta f \approx -\frac{\tau}{\hbar} (1 - \mathbb{P}) \nabla_k \mathcal{E} \cdot \left( \nabla_r T \partial_T - (e\mathbf{E} - \nabla_r \mu) \partial_{\mathcal{E}} \right) f_{\text{ieq}}. \quad (\text{C8})$$

We now consider the contributions to  $\delta f$  which are independent of  $\mathbb{P}$  and then those which are dependent on  $\mathbb{P}$ .

**Contributions independent of  $\mathbb{P}$ :** We now consider the contribution to  $\delta f$  which is independent of  $\mathbb{P}$ . Its contribution to the electric conductivity is

$$\sigma_{ij}(\mathbf{r}) = -\frac{e^2 \tau}{\hbar^2} \sum_{\pm} \int_{\mathbf{k}} (\partial_{k_i} \mathcal{E}_{\pm}) (\partial_{k_j} \mathcal{E}_{\pm}) \partial_{\mathcal{E}} f_{\text{ieq}}. \quad (\text{C9})$$

This expression is symmetric in the indices  $i$  and  $j$ . Thus, this term can only contribute to the symmetric part of the electric conductivity. The same argument follows for the thermoelectric and thermal conductivities. The leading order contribution in this regime is giving by Eq. (46).

**Contributions dependent on  $\mathbb{P}$ :** Extrinsic contributions to the totally antisymmetric pieces to the conductivities must arise from the terms including  $\mathbb{P}$  in  $\delta f$ . The operator  $\mathbb{P}$  contains  $\nabla_r$  and  $\nabla_k$  which act on every term to the right of  $\mathbb{P}$ . We argue that the derivatives  $\nabla_k$  and  $\partial_{\mathcal{E}}$  on  $(\nabla_r T \partial_T - (e\mathbf{E} - \nabla_r \mu) \partial_{\mathcal{E}}) f_{\text{ieq}}$  are sub leading order and thus we only consider derivatives that act on  $\nabla_k \mathcal{E}$ . Due to this action the terms proportional to  $\dot{\mathbf{r}}^{(0)}$  in  $\mathbb{P}$  are largely suppressed in  $\delta f$ .

This leads to the largest terms in  $\delta f$  appearing from terms in  $\mathbb{P}$  that are second order in our small parameters and deriving from  $\dot{\mathbf{k}}^{(1)}$ . First, we consider terms which scale in  $\mathbb{P}$  like  $(\ell/L_s)(\lambda/t)$ . We find

$$\begin{aligned} \delta f^{(\lambda^1)} &\approx -\frac{\tau^2}{\hbar^2} (\nabla_r \mathcal{E} \cdot \nabla_k) \nabla_k \mathcal{E} \cdot \left( \nabla_r T \partial_T - (e\mathbf{E} - \nabla_r \mu) \partial_{\mathcal{E}} \right) f_{\text{ieq}} \\ &\approx -\frac{\hbar \tau^2 \lambda}{at} (\partial_{r_i} \hat{m}_i) \chi_{ji} v_j M_{ln}^{-1} \left( \partial_{r_n} T \partial_T - (eE_n - \partial_{r_n} \mu) \partial_{\mathcal{E}} \right) f_{\text{ieq}} \end{aligned} \quad (\text{C10})$$

where the second line used the expansion of the energy (C7) to first order in  $\lambda$ . Adopting the notation  $\zeta \in \{\sigma, \alpha, \kappa\}$ , the contribution to the conductivities which arises from  $\delta f^{(\lambda^1)}$  is

$$\zeta_{mn} = \frac{\hbar \tau^2 \lambda}{at} \sum_{\pm} \int_{\mathbf{k}} s \chi_{ji} v_j M_{ln}^{-1} v_m (\partial_{\varepsilon} X_{\pm}^{\zeta}) \int_{\mathbf{r}} \partial_{r_i} \hat{m}_i \quad (\text{C11})$$

where  $X^\zeta$  is defined in eq. (43). The total derivative in the real space integral would vanish for periodic textures and at most is a boundary contribution to the conductivities. As a reminder these terms scale in  $\mathbb{P}$  as  $(\ell/L_s)(\lambda/t)$ . We next turn to the terms in  $\mathbb{P}$  which scale like  $(\ell/L_s)(a/L_s)$ .

Letting  $\lambda = 0$ , spatial derivatives on the energy vanish and  $\mathcal{E}_\pm(\boldsymbol{\xi}) = \varepsilon_\pm(\mathbf{k})$ . We therefore find that  $\mathbb{P} \approx \tau \dot{\mathbf{k}}_{\lambda=0}^{(0)} \cdot \nabla_{\mathbf{k}}$ , where  $(\dot{\mathbf{k}}_{\lambda=0}^{(0)})_i = (\Omega_{r_i r_j} - (e/\hbar)F_{ij})\partial_{k_j}\varepsilon/\hbar$ . The largest term in this limit in  $\delta f$  arising from  $\mathbb{P}$  is

$$\delta f^{(\lambda^0)} = \hbar\tau^2 \left( \Omega_{r_i r_j} - \frac{e}{\hbar}F_{ij} \right) v_j M_{im}^{-1} \left( \partial_{r_m} T \partial_T - (eE_m - \partial_{r_m}\mu)\partial_\varepsilon \right) f_{\text{eq}}. \quad (\text{C12})$$

Recall that  $\partial_T f_{\text{eq}} = -(\varepsilon - \mu_0)/T_0 \partial_\varepsilon f_{\text{eq}}$ . Thus, the final expression for the  $\tau^2$  term is

$$\delta f^{(\lambda^0)} = -\hbar\tau^2 \left( \Omega_{r_i r_j} - \frac{e}{\hbar}F_{ij} \right) v_j M_{im}^{-1} \left( \frac{(\varepsilon - \mu_0)}{T_0} \partial_{r_m} T + (eE_m - \partial_{r_m}\mu) \right) \partial_\varepsilon f_{\text{eq}}. \quad (\text{C13})$$

#### Appendix D: Relating Equilibrium Current to Bound Current

We start with the expression in Eq. (32). In global equilibrium, the distribution function is the Fermi-Dirac distribution, and  $\dot{\mathbf{r}}^{(0)}$  is given by Eq. (12) without the electric field. We have

$$\begin{aligned} \mathbf{j}_{\text{eq}}^e(\mathbf{r}) &= -e \sum_{\pm} \int_{\mathbf{k}} \left[ \mathcal{D}f_{\text{eq}}(\boldsymbol{\xi}) \dot{\mathbf{r}}^{(0)} + \nabla_{\mathbf{r}} \times \left( \mathcal{D}f_{\text{eq}}(\boldsymbol{\xi}) \mathbf{m}(\boldsymbol{\xi}) \right) \right] \\ \mathbf{j}_{\text{eq}}^Q(\mathbf{r}) &= \sum_{\pm} \int_{\mathbf{k}} \left[ \mathcal{D}f_{\text{eq}}(\boldsymbol{\xi}) \dot{\mathbf{r}}^{(0)} (\mathcal{E} - \mu_0) + \nabla_{\mathbf{r}} \times \left( \mathcal{D}f_{\text{eq}}(\boldsymbol{\xi}) (\mathcal{E} - \mu_0) \mathbf{m}(\boldsymbol{\xi}) \right) \right] \end{aligned} \quad (\text{D1})$$

Our goal is to manipulate the equilibrium currents so that they take a manifestly solenoidal form:  $\mathbf{j} \sim \nabla \times \mathcal{F}$  for some vector field  $\mathcal{F}$ . Since the second terms in both currents are already written in this manner, we only need to focus on rewriting the first terms. Let us first focus on the electric current. Recall that  $\partial g_{\text{eq}}/\partial \mathcal{E} = f_{\text{eq}}$  and  $(\partial/\partial \mathcal{E})(h_{\text{eq}} - \mu_0 g_{\text{eq}}) = (\mathcal{E} - \mu_0)f_{\text{eq}}$ . We have

$$\begin{aligned} \left( -e \int_{\mathbf{k}} \mathcal{D}(\partial_{\mathcal{E}} g_{\text{eq}}) \dot{\mathbf{r}}^{(0)} \right)_i &= -\frac{e}{\hbar} \int_{\mathbf{k}} \left( \mathbf{K}_{ij} \partial_{r_j} \mathcal{E} \partial_{\mathcal{E}} g_{\text{eq}} + \mathbf{S}_{ij} \partial_{k_j} \mathcal{E} \partial_{\mathcal{E}} g_{\text{eq}} \right) \\ &= -\frac{e}{\hbar} \int_{\mathbf{k}} \left( \mathbf{K}_{ij} \partial_{r_j} g_{\text{eq}} + \mathbf{S}_{ij} \partial_{k_j} g_{\text{eq}} \right) \end{aligned} \quad (\text{D2})$$

We use the chain rule to rewrite these terms:

$$\begin{aligned} \mathbf{K}_{ij} \partial_{r_j} g_{\text{eq}} &= \partial_{r_j} (\mathbf{K}_{ij} g_{\text{eq}}) - (\partial_{r_j} \mathbf{K}_{ij}) g_{\text{eq}} \\ \mathbf{S}_{ij} \partial_{k_j} g_{\text{eq}} &= \partial_{k_j} (\mathbf{S}_{ij} g_{\text{eq}}) - (\partial_{k_j} \mathbf{S}_{ij}) g_{\text{eq}} \end{aligned} \quad (\text{D3})$$

The term  $\partial_{k_j} (\mathbf{S}_{ij} g_{\text{eq}})$  can be neglected in the integral because the Brillouin zone has no boundary. To leading order in the curvatures  $\mathbf{K}_{ij} \approx \Omega_{k_i k_j}$ , which affords us the relation  $\partial_{r_j} \mathbf{K}_{ij} = -\partial_{k_j} \mathbf{S}_{ij}$ . Using these results we have

$$-e \int_{\mathbf{k}} \mathcal{D}(\partial_{\mathcal{E}} g_{\text{eq}}) \dot{\mathbf{r}}^{(0)} \approx -\frac{e}{\hbar} \partial_{r_j} \int_{\mathbf{k}} (\Omega_{k_i k_j} g_{\text{eq}}) \quad (\text{D4})$$

Writing the antisymmetric k-space Berry curvature in its vector form we may express the electric charge current as

$$\mathbf{j}_{\text{eq}}^e(\mathbf{r}) = -\frac{e}{\hbar} \nabla_{\mathbf{r}} \times \sum_{\pm} \int_{\mathbf{k}} \left( g_{\text{eq}} \boldsymbol{\Omega}_{\mathbf{k}} + \hbar \mathcal{D}f_{\text{eq}} \mathbf{m} \right) \quad (\text{D5})$$

The analysis proceeds in the same way for the thermal currents, with  $(h_{\text{eq}} - \mu_0 g_{\text{eq}})$  in this case taking the place of  $g_{\text{eq}}$ .

### Appendix E: Anomalous Transport Coefficients

In this appendix, we show how the anomalous Hall transport coefficients can be rewritten to assume the form shown in Eq. (49). We show the calculation for the anomalous Hall conductivity as an example. Starting with the expression for the anomalous contribution to  $\sigma_H$  from Eq. (47):

$$\sigma_i^A = -\frac{e^2}{\hbar} \sum_{\pm} \int_{\xi} f_{\text{eq}} \Omega_{k_i} \quad (\text{E1})$$

We substitute the expression for the k-space Berry curvature, to lowest order in  $(\lambda/J)$ :

$$\begin{aligned} \Omega_{k_i} &= \frac{1}{2} \epsilon_{ijk} \Omega_{k_j k_k} = \frac{1}{4} \epsilon_{ijk} \epsilon_{lmn} \hat{d}_l (\partial_{k_j} \hat{d}_m) (\partial_{k_k} \hat{d}_n) \\ &= -\frac{\hbar^4}{4} \left( \frac{\lambda}{Jat} \right)^2 \epsilon_{ijk} \epsilon_{lmn} \hat{m}_l(\mathbf{r}) \chi_{m\mu} \chi_{n\nu} M_{j\mu}^{-1} M_{k\nu}^{-1} \end{aligned} \quad (\text{E2})$$

At this order of the calculation, the only spatial dependence is coming from the magnetic texture in the berry curvature. Noting that the elements of  $\overline{\chi}$  are constants, we find

$$\sigma_i^A = \frac{e^2 \hbar^3}{4} \left( \frac{\lambda}{Jat} \right)^2 \epsilon_{ijk} \epsilon_{lmn} \chi_{m\mu} \chi_{n\nu} \sum_{\pm} \int_{\mathbf{r}} \hat{m}_l(\mathbf{r}) \int_{\mathbf{k}} f_{\text{eq}} M_{j\mu}^{-1} M_{k\nu}^{-1} \quad (\text{E3})$$

We focus on manipulating the k-space integral:

$$f_{\text{eq}} M_{j\mu}^{-1} M_{k\nu}^{-1} = \frac{1}{\hbar^2} \left[ \partial_{k_j} (f_{\text{eq}} v_{\mu} \partial_{k_k} v_{\nu}) - (\partial_{k_j} f_{\text{eq}}) v_{\mu} \partial_{k_k} v_{\nu} - f_{\text{eq}} v_{\mu} (\partial_{k_j} \partial_{k_k} v_{\nu}) \right] \quad (\text{E4})$$

The first term vanishes upon integrating over k-space. The term containing  $\partial_{k_j} \partial_{k_k} v_{\mu}$  is symmetric in the  $j, k$  indices. Combined with the antisymmetric  $\epsilon_{ijk}$ , this term must also vanish. Thus, the k-space integral becomes

$$\int_{\mathbf{k}} f_{\text{eq}} M_{j\mu}^{-1} M_{k\nu}^{-1} = -\frac{1}{\hbar} \int_{\mathbf{k}} (\partial_{k_j} f_{\text{eq}}) v_{\mu} M_{k\nu}^{-1} \quad (\text{E5})$$

We note that  $\partial_{k_j} f_{\text{eq}} = \hbar v_j \partial_{\varepsilon} f_{\text{eq}}$  such that we may express the anomalous contribution to the electric conductivity as

$$\sigma_i^A = -\frac{e^2 \hbar^3}{4} \left( \frac{\lambda}{Jat} \right)^2 \epsilon_{ijk} \epsilon_{lmn} \chi_{m\mu} \chi_{n\nu} \sum_{\pm} \int_{\mathbf{r}} \hat{m}_l(\mathbf{r}) \int_{\mathbf{k}} (\partial_{\varepsilon} f_{\text{eq}}) v_j M_{k\nu}^{-1} v_{\mu} \quad (\text{E6})$$

Next, we use  $\epsilon_{lmn} \chi_{m\mu} \chi_{n\nu} = -\epsilon_{lmn} \chi_{n\mu} \chi_{m\nu}$ , which allows us to write  $\epsilon_{lmn} \chi_{m\mu} \chi_{n\nu} = \frac{1}{2} \epsilon_{lmn} \epsilon_{\gamma\alpha\beta} \epsilon_{\gamma\mu\nu} \chi_{m\alpha} \chi_{n\beta}$ . Inserting this into our expression for the conductivity,

$$\sigma_i^A = -\frac{e^2 \hbar^3}{8} \left( \frac{\lambda}{Jat} \right)^2 \epsilon_{ijk} \epsilon_{lmn} \epsilon_{\gamma\alpha\beta} \epsilon_{\gamma\mu\nu} \chi_{m\alpha} \chi_{n\beta} \sum_{\pm} \int_{\mathbf{r}} \hat{m}_l(\mathbf{r}) \int_{\mathbf{k}} (\partial_{\varepsilon} f_{\text{eq}}) v_j M_{k\nu}^{-1} v_{\mu} = F_{il} \Lambda_l \quad (\text{E7})$$

where  $\Lambda$  is defined in Eq. (56). The procedure for expressing  $\alpha_H^A$  and  $\kappa_H^A$  in this form follows from a similar analysis.

### Appendix F: Kelvin, Wiedemann-Franz, and Mott Relations

The full expressions (including both longitudinal and transverse parts) for the transport coefficients are

$$\begin{aligned} \sigma_{lm} &= -e^2 \sum_{\pm} \int_{\xi} \left[ \tau \left( v_m - \hbar \tau \sum_{ij} (s\Omega_{r_i r_j} - \frac{e}{\hbar} F_{ij}) v_j M_{im}^{-1} \right) \left( \partial_{\varepsilon} f_{\text{eq}} \right) v_l + \epsilon_{lnm} s \frac{\Omega_{k_n}}{\hbar} \partial_{\mu_0} g_{\text{eq}} \right] \\ \alpha_{lm} &= e \sum_{\pm} \int_{\xi} \left[ \tau \left( v_m - \hbar \tau \sum_{ij} (s\Omega_{r_i r_j} - \frac{e}{\hbar} F_{ij}) v_j M_{im}^{-1} \right) \left( \frac{(\varepsilon - \mu_0)}{T_0} \partial_{\varepsilon} f_{\text{eq}} \right) v_l + \epsilon_{lnm} s \frac{\Omega_{k_n}}{\hbar} \partial_{T_0} g_{\text{eq}} \right] \\ \beta_{lm} &= e \sum_{\pm} \int_{\xi} \left[ \tau \left( v_m - \hbar \tau \sum_{ij} (s\Omega_{r_i r_j} - \frac{e}{\hbar} F_{ij}) v_j M_{im}^{-1} \right) \left( (\varepsilon - \mu_0) \partial_{\varepsilon} f_{\text{eq}} \right) v_l + \epsilon_{lnm} s \frac{\Omega_{k_n}}{\hbar} T_0 \partial_{T_0} g_{\text{eq}} \right] \\ \kappa_{lm} &= -\sum_{\pm} \int_{\xi} \left[ \tau \left( v_m - \hbar \tau \sum_{ij} (s\Omega_{r_i r_j} - \frac{e}{\hbar} F_{ij}) v_j M_{im}^{-1} \right) \left( \frac{(\varepsilon - \mu_0)^2}{T_0} \partial_{\varepsilon} f_{\text{eq}} \right) v_l + \epsilon_{lnm} s \frac{\Omega_{k_n}}{\hbar} \partial_{T_0} (h_{\text{eq}} - \mu_0 g_{\text{eq}}) \right] \end{aligned} \quad (\text{F1})$$

where for simplicity we have suppressed the dependence of various quantities on the band index  $s = \pm$  and phase space variables  $\xi$ . The Kelvin relation ( $\vec{\beta} = T_0 \vec{\alpha}$ ) is clearly seen from the expressions above.

**Wiedemann-Franz.** The Wiedemann-Franz relationship states that  $\vec{\kappa} \approx \frac{\pi^2}{3} \frac{k_B^2 T}{e^2} \vec{\sigma}$ . We start by comparing the intrinsic contributions

$$\kappa_{lm}^{(\text{int})} = -\frac{1}{\hbar} \sum_{\pm} \int_{\xi} \partial_{T_0} (h_{\text{eq}} - \mu_0 g_{\text{eq}}) \epsilon_{lnm} s \Omega_{k_n}; \quad \sigma_{lm}^{(\text{int})} = -\frac{e^2}{\hbar} \sum_{\pm} \int_{\xi} \partial_{\mu_0} g_{\text{eq}} \epsilon_{lnm} s \Omega_{k_n}. \quad (\text{F2})$$

First we rewrite  $\kappa_{lm}^{(\text{int})}$  as

$$\kappa_{lm}^{(\text{int})} = -\frac{1}{\hbar} \sum_{\pm} \int d\eta \int_{\xi} \partial_{T_0} \left( h_{\text{eq}}(\eta) - \mu_0 g_{\text{eq}}(\eta) \right) \partial_{\eta} \Theta(\eta - \varepsilon) \epsilon_{lnm} s \Omega_{k_n}, \quad (\text{F3})$$

where  $\Theta(x)$  is the Heaviside step function, and integrate by parts to write  $\kappa_{lm}^{(\text{int})}$  in terms of a function  $G_{lm}(\eta)$  as

$$\kappa_{lm}^{(\text{int})} = \sum_{\pm} \int d\eta G_{lm}(\eta) \partial_{T_0} f_{\text{eq}}(\eta) (\eta - \mu_0) \quad (\text{F4})$$

with

$$G_{lm}(\eta) = \frac{1}{\hbar} \int_{\xi} \Theta(\eta - \varepsilon) \epsilon_{lnm} s \Omega_{k_n}. \quad (\text{F5})$$

Similarly, we may write  $\sigma_{lm}^{(\text{int})}$  as

$$\sigma_{lm}^{(\text{int})} = -e^2 \sum_{\pm} \int d\eta G_{lm}(\eta) \partial_{\eta} f_{\text{eq}}(\eta). \quad (\text{F6})$$

Next, we note that derivatives with respect to  $T_0$  and  $\eta$  of  $f_{\text{eq}}(\eta)$  satisfy the relation  $\partial_{T_0} f(\eta) = -(\eta - \mu_0) \partial_{\eta} f(\eta) / T_0$ . At low temperatures  $k_B T_0 \ll E_F$ , the function  $\partial_{\eta} f_{\text{eq}}(\eta)$  is sharply peaked in the small region of width  $k_B T_0$  about  $\mu_0$ . We therefore perform a low temperature expansion around  $\mu_0$ . The intrinsic contributions can be expanded as follows:

$$\begin{aligned} \kappa_{lm}^{(\text{int})} &= -\sum_{\pm} \int d\eta \left[ G_{lm}(\mu_0) + (\eta - \mu_0) \partial_{\mu_0} G_{lm} \right] \frac{(\eta - \mu_0)^2}{T_0} \partial_{\eta} f_{\text{eq}}(\eta) + \dots \\ \sigma_{lm}^{(\text{int})} &= -e^2 \sum_{\pm} \int d\eta \left[ G_{lm}(\mu_0) + (\eta - \mu_0) \partial_{\mu_0} G_{lm} \right] \partial_{\eta} f_{\text{eq}}(\eta) + \dots \end{aligned} \quad (\text{F7})$$

The term involving  $(\eta - \mu_0)^3$  in  $\kappa_{lm}^{(\text{int})}$  and the term involving  $(\eta - \mu_0)$  in  $\sigma_{lm}^{(\text{int})}$  both vanish upon integration. The expressions are thus approximately

$$\begin{aligned} \kappa_{lm}^{(\text{int})} &\approx -\sum_{\pm} G_{lm}(\mu_0) \int d\eta \frac{(\eta - \mu_0)^2}{T_0} \partial_{\eta} f_{\text{eq}}(\eta) = -k_B^2 T_0 \frac{\pi^2}{3} \sum_{\pm} G_{lm}(\mu_0) \\ \sigma_{lm}^{(\text{int})} &\approx -e^2 \sum_{\pm} G_{lm}(\mu_0) \int d\eta \partial_{\eta} f_{\text{eq}}(\eta) = -e^2 \sum_{\pm} G_{lm}(\mu_0). \end{aligned} \quad (\text{F8})$$

Note the relationship between the expressions for  $\kappa_{lm}^{(\text{int})}$  and  $\sigma_{lm}^{(\text{int})}$ .

Next, we analyze the extrinsic contributions:



$$\begin{aligned}
\sigma_{lm}^{(\text{ext})} &= -e^2 \sum_{\pm} \int_{\xi} \left[ \tau \left( v_m - \hbar\tau \sum_{ij} (s\Omega_{r_i r_j} - \frac{e}{\hbar} F_{ij}) v_j M_{im}^{-1} \right) \left( \partial_{\varepsilon} f_{\text{eq}} \right) v_l \right] \\
\kappa_{lm}^{(\text{ext})} &= - \sum_{\pm} \int_{\xi} \left[ \tau \left( v_m - \hbar\tau \sum_{ij} (s\Omega_{r_i r_j} - \frac{e}{\hbar} F_{ij}) v_j M_{im}^{-1} \right) \left( \frac{(\varepsilon - \mu_0)^2}{T_0} \partial_{\varepsilon} f_{\text{eq}} \right) v_l \right].
\end{aligned} \tag{F9}$$

We rewrite these contributions in terms of a function  $G'_{lm}(\eta)$  as

$$\kappa_{lm}^{(\text{ext})} = \sum_{\pm} \int d\eta G'_{lm}(\eta) \frac{(\eta - \mu_0)^2}{T_0} \partial_{\eta} f_{\text{eq}}(\eta); \quad \sigma_{lm}^{(\text{ext})} = e^2 \sum_{\pm} \int d\eta G'_{lm}(\eta) \partial_{\eta} f_{\text{eq}}(\eta) \tag{F10}$$

with

$$G'_{lm}(\eta) = - \int_{\xi} \left[ \tau \left( v_m - \hbar\tau \sum_{ij} (s\Omega_{r_i r_j} - \frac{e}{\hbar} F_{ij}) v_j M_{im}^{-1} \right) \delta(\eta - \varepsilon) \right] \tag{F11}$$

where  $\delta(x)$  is the Dirac delta function. Again, we perform a low temperature expansion. The extrinsic contributions are approximated as

$$\begin{aligned}
\kappa_{lm}^{(\text{ext})} &\approx \sum_{\pm} G_{lm}(\mu_0) \int d\eta \frac{(\eta - \mu_0)^2}{T_0} \partial_{\eta} f_{\text{eq}}(\eta) = \frac{\pi^2}{3} k_B^2 T_0 \sum_{\pm} G_{lm}(\mu_0) \\
\sigma_{lm}^{(\text{ext})} &\approx e^2 \sum_{\pm} G_{lm}(\mu_0) \int d\eta \partial_{\eta} f_{\text{eq}}(\eta) = e^2 \sum_{\pm} G_{lm}(\mu_0).
\end{aligned} \tag{F12}$$

Overall, we therefore find that the Wiedemann-Franz relation  $\kappa_{lm}/\sigma_{lm} = (\pi^2/3)(k_B^2 T_0/e^2)$  is satisfied for both the intrinsic and extrinsic contributions.

**The Mott Relation.** The Mott relation states  $\vec{\alpha} \approx -\frac{\pi^2}{3} \frac{k_B^2 T}{e} \frac{\partial}{\partial \mu_0} \vec{\sigma}$ . We shall follow a procedure similar to the one shown for the Wiedemann-Franz relation. We start by comparing the intrinsic contributions:

$$\alpha_{lm}^{(\text{int})} = \frac{e}{\hbar} \sum_{\pm} \int_{\xi} \epsilon_{lmn} s \Omega_{k_n} \partial_{T_0} g_{\text{eq}}; \quad \sigma_{lm}^{(\text{int})} = \frac{e^2}{\hbar} \sum_{\pm} \int_{\xi} \epsilon_{lmn} s \Omega_{k_n} f_{\text{eq}}. \tag{F13}$$

Following the same procedure as was used in the Wiedemann-Franz section, we rewrite  $\alpha_{lm}^{(\text{int})}$  and  $\sigma_{lm}^{(\text{int})}$  as

$$\alpha_{lm}^{(\text{int})} = -\frac{e}{\hbar} \sum_{\pm} \int d\eta \mathcal{G}_{lm}(\eta) \partial_{T_0} f_{\text{eq}}(\eta); \quad \sigma_{lm}^{(\text{int})} = -\frac{e^2}{\hbar} \sum_{\pm} \int d\eta \mathcal{G}_{lm}(\eta) \partial_{\eta} f_{\text{eq}}(\eta) \tag{F14}$$

with

$$\mathcal{G}_{lm}(\eta) = \int_{\xi} \epsilon_{lmn} s \Omega_{k_n} \Theta(\eta - \varepsilon). \tag{F15}$$

Again using the fact that  $\partial_{T_0} f_{\text{eq}}(\eta) = -(\eta - \mu_0) \partial_{\eta} f_{\text{eq}}(\eta)/T_0$ , and employing a low temperature expansion about  $\mu_0$ , we find

$$\alpha_{lm}^{(\text{int})} \approx \frac{e}{\hbar} k_B^2 T_0 \frac{\pi^2}{3} \sum_{\pm} \partial_{\mu_0} \mathcal{G}_{lm}(\mu_0); \quad \sigma_{lm}^{(\text{int})} \approx -\frac{e^2}{\hbar} \sum_{\pm} \mathcal{G}_{lm}(\mu_0). \tag{F16}$$

A similar form can be determined for the extrinsic contributions:

$$\alpha_{lm}^{(\text{ext})} = \frac{e}{\hbar} \sum_{\pm} \int d\eta \mathcal{G}'_{lm}(\eta) \frac{(\eta - \mu_0)}{T_0} \partial_{\eta} f_{\text{eq}}(\eta); \quad \sigma_{lm}^{(\text{ext})} = -\frac{e^2}{\hbar} \sum_{\pm} \int d\eta \mathcal{G}'_{lm}(\eta) \partial_{\eta} f_{\text{eq}}(\eta) \quad (\text{F17})$$

with

$$\mathcal{G}'_{lm}(\eta) = e \sum_{\pm} \int_{\xi} \tau \left( v_m - \hbar \tau \sum_{ij} (s\Omega_{r_i r_j} - \frac{e}{\hbar} F_{ij}) v_j M_{im}^{-1} \right) \delta(\eta - \varepsilon). \quad (\text{F18})$$

After the low temperature expansion, we have

$$\alpha_{lm}^{(\text{ext})} \approx \frac{e}{\hbar} \sum_{\pm} \frac{\partial \mathcal{G}'_{lm}}{\partial \mu_0} \int d\eta \frac{(\eta - \mu_0)^2}{T_0} \partial_{\eta} f_{\text{eq}}(\eta); \quad \sigma_{lm}^{(\text{ext})} \approx -\frac{e^2}{\hbar} \sum_{\pm} \mathcal{G}'_{lm}(\mu_0) \int d\eta \partial_{\eta} f_{\text{eq}}(\eta) \quad (\text{F19})$$

which integrates to

$$\alpha_{lm}^{(\text{ext})} \approx \frac{e}{\hbar} k_B^2 T_0 \frac{\pi^2}{3} \sum_{\pm} \frac{\partial \mathcal{G}'_{lm}(\mu_0)}{\partial \mu_0}; \quad \sigma_{lm}^{(\text{ext})} \approx -\frac{e^2}{\hbar} \sum_{\pm} \mathcal{G}'_{lm}(\mu_0) \quad (\text{F20})$$

We see that  $\alpha_{lm} \approx -\frac{\pi^2}{3} \frac{k_B^2 T}{e} \frac{\partial}{\partial \mu_0} \sigma_{lm}$  and the Mott relation is indeed satisfied for both the intrinsic and extrinsic contributions.

### Appendix G: Scaling Transport Coefficients

Here we take the regime of interest to be defined by the inequalities  $a \ll \ell \ll L_s$  and  $\lambda \ll J < t \sim E_F$ . The resistivity scaling shown in Table 1 derives from the approximations  $\rho_{xx} \approx (1/\sigma_{xx})$  and  $\rho_{xy} \approx \sigma_{xy}/\sigma_{xx}^2$ . The ordinary conductivities are in agreement with the usual Drude-Boltzmann results, meaning that  $\sigma_{xx} \sim (e^2/\hbar)(k_F^2 \ell)$  and  $\sigma_{xy}^O = \omega_c \tau \sigma_{xx}$ , which leads to the results for the longitudinal and ordinary Hall resistivities. The scaling of the anomalous Hall conductivity is most easily seen from Eq. (53), which leads to the scaling for the anomalous Hall resistivity. The scaling for the topological Hall conductivity is found directly from Eq. (49). Using the fact that  $n^{\text{sk}} \sim (1/L_s^2)$ , this analysis proceeds as

$$\sigma^T \sim e^2 \tau^2 \hbar \frac{1}{L_s^2} \int_{\mathbf{k}} \frac{\partial f_{\text{eq}}}{\partial \varepsilon} v^2 M^{-1} \sim \frac{e^2}{\hbar} \frac{1}{L_s^2} (\tau v_F)^2 k_F^2 a \sim \left( \frac{e^2}{\hbar} k_F \right) \left( \frac{\ell}{L_s} \right)^2, \quad (\text{G1})$$

and the topological Hall resistivity scaling follows. To determine the Seebeck and Nernst scaling, we employ the Mott relation:

$$S \sim \frac{k_B^2 T}{e} \frac{(\partial/\partial \mu) \sigma_{xx}}{\sigma_{xx}}; \quad N \sim \frac{k_B^2 T}{e} \frac{\partial}{\partial \mu} \left( \frac{\sigma_{xy}}{\sigma_{xx}} \right) \quad (\text{G2})$$

The derivative of the conductivities with respect to the chemical potential is governed by the distribution function  $f_{\text{eq}}$ . The higher the temperature  $T_0$  compared to the Fermi temperature  $T_F$ , the more electronic states are available to participate in transport. The correct factor is thus  $T_0/T_F$ . This combined with the conductivity scaling leads to the entries for  $S$  and  $N$  found in Table (1). Finally, the scaling of the thermal conductivities is determined from the Wiedemann-Franz law (see Appendix F).